2004-07-09

# Architectures for Symbol Timing Synchronization in MIMO Communications

Kejing Liu
*Brigham Young University - Provo*

# ARCHITECTURES FOR SYMBOL TIMING SYNCHRONIZATION IN MIMO COMMUNICATIONS

by

Kejing Liu

A thesis submitted to the faculty of

Brigham Young University

in partial fulfillment of the requirements for the degree of

Master of Science

Department of Electrical and Computer Engineering

Brigham Young University

August 2004

BRIGHAM YOUNG UNIVERSITY

GRADUATE COMMITTEE APPROVAL

of a thesis submitted by

Kejing Liu

This thesis has been read by each member of the following graduate committee and by majority vote has been found to be satisfactory.

| | |
|---|---|
| Date | Michael Rice, Chair |
| Date | Brian D. Jeffs |
| Date | Travis Oliphant |

BRIGHAM YOUNG UNIVERSITY

As chair of the candidate's graduate committee, I have read the thesis of Kejing Liu in its final form and have found that (1) its format, citations, and bibliographical style are consistent and acceptable and fulfill university and department style requirements; (2) its illustrative materials including figures, tables, and charts are in place; and (3) the final manuscript is satisfactory to the graduate committee and is ready for submission to the university library.

Date

Michael Rice
Chair, Graduate Committee

Accepted for the Department

Michael A. Jensen
Graduate Coordinator

Accepted for the College

Douglas M. Chabries
Dean, College of Engineering and Technology

ABSTRACT

ARCHITECTURES FOR SYMBOL TIMING SYNCHRONIZATION IN MIMO COMMUNICATIONS

Kejing Liu

Department of Electrical and Computer Engineering

Master of Science

Maximum likelihood symbol timing estimation for communication over a frequency non-selective MIMO fading channel is developed. The cases of known data (data-aided estimation) and unknown data (non-data-aided estimation) together with known channel and unknown channel are considered. The analysis shows that the log-likelihood functions and their approximations can be interpreted as SISO log-likelihood functions operating on each of the receive antennas. Previously published symbol timing estimators are shown to be special cases of the more general framework presented. Architectures based on both block processing and sequential processing using a discrete-time phase-locked loop are summarized. Performance examples over a MIMO channel based on measured data and on a simple stochastic MIMO channel model are given. These examples show that the mean-squared error performance of these techniques is not strongly dependent on the MIMO channel and is able to reach the Cramér-Rao bound when sufficient complexity is applied.

# ACKNOWLEDGMENTS

This work was funded by the National Science Foundation under Information Technology Research Grant CCR-0081476 and the T&E S&T Spectrum Efficient Technologies Program under U.S. Air Force Grant DOD ARTM F04611-02-C-0020. First, I thank my advisor, Professor Michael Rice, for the hours that he spent with me in producing my thesis. I acknowledge the help from other faculty members and the support that I received from the Department of the Electrical and Computer Engineering at Brigham Young University. I would also like to thank Julie Carver for helpful discussions on my English writing. At last, I thank my husband, Jikun Liu, for his support to help me produce my thesis.

# Contents

# List of Figures

# Chapter 1

# INTRODUCTION

## 1.1 Introduction

The use of multiple transmit and receive antennas over multiple-input multiple-output (MIMO) multipath fading channels has received considerable attention due to its promise of increased channel capacity. In these systems, different data streams are transmitted in parallel over multiple transmit antennas to exploit the potential increases in capacity offered by the presence of multipath propagation. Space-time coding is used to impose structure on the transmitted data streams [1, 2, 3, 4, 5, 6], and that structure is used by the receiver to recover the data from the received signals. The signal processing and channel estimation functions described in these papers work on the matched filter outputs at each of the receive antennas. An implicit assumption is that symbol timing synchronization has already been achieved.

Underlying the space-time codes is a modulation format that is used to convey the information from the multiple transmit antennas to the multiple receive antennas. Most of the coding schemes envision the same modulation format operating on all the transmit antennas. The symbol-timing problem for MIMO systems using space-time coding was discussed briefly in [7]. This development assumes orthogonal training sequences and exploits the orthogonality to simplify an approximate Maximum Likelihood error signal. A simple search algorithm is used to find the optimum sampling instant in an oversampled data stream.

This thesis develops four maximum likelihood symbol timing estimators assuming linear modulation with a common pulse shape and frequency non-selective

fading. Maximum likelihood estimation is a way to estimate the unknown parameter by using the probability density function. No assumption regarding orthogonality is required. The frequency non-selective fading assumption means there is no time dispersion over the channel, so the optimum matched filter sampling time is the same across the entire receive antenna array. The first maximum likelihood symbol timing estimator discussed is for a data-aided and known channel system, the second one is for a data-aided and unknown channel system, the third one is for a non-data-aided and known channel system, and the last one is for a non-data-aided and unknown channel system. For these four different conditional maximum likelihood symbol timing estimators, the known channel system or data is used to estimate the unknown data or unknown channel system. Then the known or estimated channel system and data are used to estimate the unknown symbol timing delay. After the maximum likelihood symbol timing delay estimator is derived, two implementations of it are discussed. The first is the closed-loop estimator suggested by an iterative (or recursive) solution to the maximum likelihood timing estimate equation. This closed-loop estimator takes the form of the familiar phase-locked loop for symbol timing control. The second implementation is an open-loop process that is appropriate for "block processing." A $Q$-stage polyphase filterbank is used to produce, in parallel, error signals for $Q$ different delays. The delay corresponding to the smallest error signal is used to recover the data for subsequent processing. The signal processing and channel estimation functions described in this thesis work on the matched filter outputs of the receive antennas.

This thesis derives the Cramer-Rao bound for the maximum likelihood symbol timing estimator and compares the mean square error of the timing estimator to the Cramer-Rao Bound.

## 1.2 Preliminaries

### 1.2.1 Notation

$N_T$ = the number of transmit antennas.

$N_R$ = the number of receive antennas.

$T_s$ = symbol time (reciprocal of the symbol rate).

$s_i(t)$ = the signal transmitted from antenna $i$ for $i = 1, 2, \ldots, N_T$.

$r_m(t)$ = the signal received on antenna $m$ for $m = 1, 2, \ldots, N_R$.

$h_{m,i}$ = the complex channel gain between transmit antenna $i$ and receive antenna $m$.

$T_0$ = the observation interval (in seconds) during which the estimate is to be made. The observation interval may also be expressed as $T_0 = L_0 T_s$.

$L_0$ = the length of the data sequence measured in symbols.

$a_i(k)$ = the $k$-th data symbol transmitted from antenna $i$ for $i = 1, 2, \ldots, N_T$. Note that the interval $0 \leq t \leq L_0 T_s$ contains contributions from symbols $a_i(-L_p), \ldots, a_i(L_0 + L_p - 1)$. Thus the range of values for the symbol index $k$ are $-L_p, -L_p + 1, \ldots, L_0 + l_p - 1$.

$p(t)$ = a unit energy pulse shape used to transmit the data symbols on the waveform channel. The pulse shape has support on the interval $-L_p T_s \leq t \leq L_p T_s$.

### 1.2.2 System Model

This thesis considers an $N_T \times N_R$ MIMO system consisting of $N_T$ transmit antennas and $N_R$ receive antennas as illustrated in Figure 1.1. The $N_T \times N_R$ MIMO system is characterized by the channel matrix $\mathbf{H}$. For the case of a frequency non-selective MIMO multipath channel, $\mathbf{H}$ is an $N_R \times N_T$ matrix consisting of complex valued channel gains $h_{m,i}$ for $i = 1, 2, \ldots, N_T$ and $m = 1, 2, \ldots, N_R$. Often, the channel gains are modeled as normalized complex Gaussian random variables [1, 5, 6, 7]. Since the channel gains do not impose any time dispersion on the received signal,

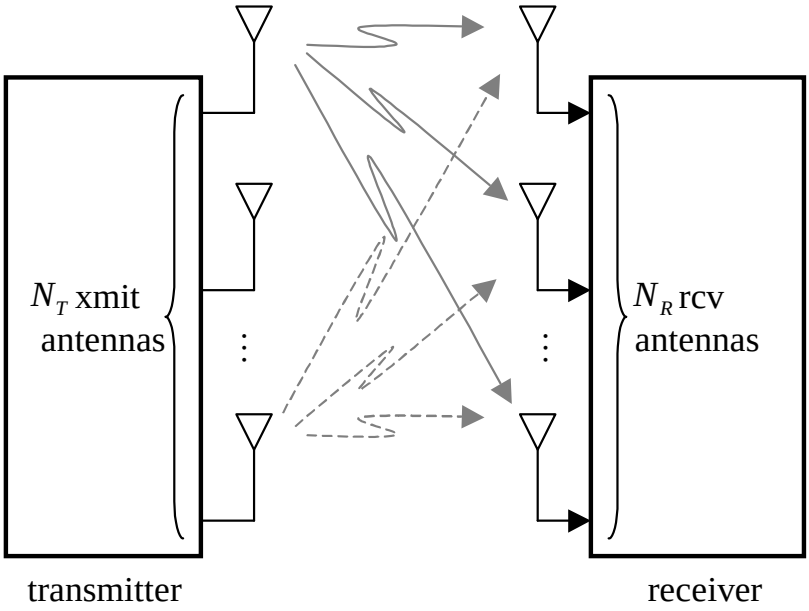


Figure 1.1: A $N_T \times N_R$ MIMO system.

the symbol timing delay is the same across all the receive antennas. This feature will be exploited to derive a timing estimator that jointly uses outputs from all the receive antennas to estimate the common timing offset.

A different data stream is transmitted from each of the transmit antennas. Assuming a common pulse shape across all $N_T$ transmit antennas, the complex baseband equivalent signal transmitted from antenna $m$ during the interval $0 \leq t \leq (L_0 T_s)$ is

$$s_i(t) = \sum_{k=-L_p}^{L_0+L_p-1} a_i(k) p\left(t - kT_s\right). \tag{1.1}$$

The temporal relationship (indexed by $k$) and spatial relationship (indexed by $i$) between the data symbols $a_i(k)$ is determined by the space-time code used for data transmission.

The $N_T$ signals are transmitted in parallel over the frequency non-selective MIMO channel characterized by a set of complex channel gains $h_{m,i}$ which represents the attenuation and phase shift between transmit antenna $i$ and receive antenna $m$. Since the channel is assumed to be frequency non-selective, there is no appreciable temporal dispersion in the received waveforms so the symbol timing delay $\tau$ can be

assumed to be the same across all receive antennas. The signal received on antenna $m$ (for $m = 1, 2, \ldots, N_R$) is

$$r_m(t) = \sum_{i=1}^{N_T} h_{m,i} s_i(t - \tau) + w_m(t), \tag{1.2}$$

where $\tau$ is the unknown symbol timing delay to be estimated and $w_m(t)$ the thermal noise contributed by the $m$-th receive antenna in the array. The thermal noise is modeled as a zero mean, complex-valued Gaussian random process whose real and imaginary parts have power spectral density $N_0/2$ Watts/Hz. The set of $N_R$ received waveforms can be represented by the vector

$$\mathbf{r}(t) = \begin{bmatrix} r_1(t) & r_2(t) & \cdots & r_{N_R}(t) \end{bmatrix}^T, \tag{1.3}$$

which can be expressed as

$$\mathbf{r}(t) = \mathbf{H}\mathbf{s}(t - \tau) + \mathbf{w}(t) \tag{1.4}$$

where

$$\mathbf{H} = \begin{bmatrix} h_{1,1} & h_{1,2} & \cdots & h_{1,N_T} \\ h_{2,1} & h_{2,2} & \cdots & h_{2,N_T} \\ \vdots & \vdots & \ddots & \vdots \\ h_{N_R,1} & h_{N_R,2} & \cdots & h_{N_R,N_T} \end{bmatrix}, \tag{1.5}$$

$$\mathbf{s}(t - \tau) = \begin{bmatrix} s_1(t - \tau) \\ s_2(t - \tau) \\ \vdots \\ s_{N_T}(t - \tau) \end{bmatrix}, \tag{1.6}$$

and

$$\mathbf{w}(t) = \begin{bmatrix} w_1(t) \\ w_2(t) \\ \vdots \\ w_{N_R}(t) \end{bmatrix}. \tag{1.7}$$

It is convenient to collect the $N_T$ data sequences into the matrix

$$\mathbf{A} = \begin{bmatrix} a_1(-L_p) & \cdots & a_1(L_0+L_p-1) \\ a_2(-L_p) & \cdots & a_2(L_0+L_p-1) \\ \vdots & \ddots & \vdots \\ a_{N_T}(-L_p) & \cdots & a_{N_T}(L_0+L_p-1) \end{bmatrix}. \tag{1.8}$$

Then

$$\mathbf{s}(t-\tau) = \mathbf{AP}(t;\tau), \tag{1.9}$$

where

$$\mathbf{P}(t;\tau) = \begin{bmatrix} p(t-(-L_p)T_s-\tau) \\ p(t-(-L_p+1)T_s-\tau) \\ \vdots \\ p(t-(L_0+L_p-1)T_s-\tau) \end{bmatrix}. \tag{1.10}$$

The set of $N_R$ received waveforms can be expressed as

$$\mathbf{r}(t) = \mathbf{HAP}(t-\tau) + \mathbf{w}(t). \tag{1.11}$$

### 1.3 Maximum Likelihood Estimation

The maximum likelihood estimation method is used to find the timing estimator. Maximum likelihood estimation is a probabilistic estimation method which chooses for the estimate, the value of that maximizes the likelihood function.

The likelihood function is based on the probability of the observed samples given the parameter to be estimated. For complete data, the likelihood function is the joint probability density function of the data. As stated in [9],

> The likelihood function $l(\theta)$ of the random variables $X_1, X_2, ...., X_n$ is the joint probabilty density function $f_{X_1,X_2,....,X_n}(x_1, x_2, ...., x_n; \theta)$ considered as a function of the unknown parameter $\theta$. In particular, if $X_1, X_2, ...., X_n$ are independent observations on a random variable $X$ with pdf $f_X(x;\theta)$, then the likelihood function becomes
>
> $$l_\theta = \prod_{i=1}^{n} f_X(x_i;\theta) \tag{1.12}$$

since the $X_i$ are i.i.d. random variable with pdf $f_X(x, \theta)$. If, for a given outcome $\mathbf{x} = (x_1, x_2, ...., x_n)$, $\hat{\theta}(x_1, x_2, ...., x_n)$ is the value of $\theta$ that maximizes $l(\theta)$, then $\hat{\theta}(x_1, x_2, ...., x_n)$ is the maximum likelihood estimator for $\theta$.

For the exponential family of probability density functions, it is simpler to use the natural log of the likelihood function, which is called the log-likelihood function. The log-likelihood function is $\Lambda_X(\theta) = \log \prod_{i=1}^{n} f_X(x_i; \theta)$. After the log-likelihood function as a function of the unknown parameter $\theta$ is found, it is differentiated with respect to the unknown parameter to find its maximum likelihood estimator.

As introduced before, the thermal noise at the received antennas, $w_m(t)$, are modeled as Gaussian i.i.d. random variables. We can write $w_m(t) = r_m(t) - \sum_{i=1}^{N_T} h_{m,i} s_i(t - \tau)$, where $\tau$ is the unknown symbol timing delay. This thesis denotes the estimator for the symbol timing delay as $\hat{\tau}$, and the received signal for a given symbol timing delay estimator is $\hat{r}_m(t) = \sum_{i=1}^{N_T} h_{m,i} s_i(t - \hat{\tau}) + w_m(t)$. Actually $r_m(t)$ is the realization of $\hat{r}_m(t)$ when $\hat{\tau} = \tau$. When $\hat{\tau}$ varies, the value of $\hat{r}_m(t)$ varies also. The maximum likelihood estimator $\tau_{ML}$ is the value of $\hat{\tau}$ which minimizes the difference between $\hat{r}_m(t)$ and $r_m(t)$.

After the maximum likelihood estimator for symbol timing delay is found, $\tau_{ML}$, its accuracy should be tested. In this thesis, one method used to test the accuracy of the maximum likelihood estimator is the mean square error. Maximum likelihood estimator is asymptotically unbiased and efficient. The Cramer Rao bound is the lower limit to the variance of unbiased estimator. The mean square error is the expected value of the square of the error of the estimator, which is a common way to measure the performance of the symbol timing delay estimator. By definition, "An estimator $\hat{\Theta}$ is called a mean-square error (MSE) estimator if

$$E[(\hat{\Theta} - \theta)^2] \leq E[(\hat{\Theta}' - \theta)^2], \tag{1.13}$$

where $\hat{\Theta}'$ is any other estimator [9]." The MSE for the symbol timing delay estimator is calculated at different signal to noise ratio (SNR) values and used to see how noise affects the performance of the timing delay estimator.

## 1.4 Cramer Rao Bound

The conditional Cramer Rao bound (CCRB) and the modified Cramer Rao bound (MCRB) can be used to find the efficiency of different estimators. The Cramer Rao bound is the minimum bound for the unbiased estimator. By looking at how close the mean square error is to the Cramer Rao bound, the efficiency of the symbol timing delay estimator can be seen.

The estimate of the symbol timing delay depends on the observations of the received signal. Different observations will change the value of the estimate. In other words, the estimate of the symbol timing delay will be distributed around the true value of the unknown symbol timing delay. The Cramer Rao bound finds the minimum variance of the error between the estimated and the true symbol timing delays.

The Cramer Rao bound is a fundamental limit for the variance of any estimator. The Cramer Rao bound is based on the Fisher information matrix, which is defined as

$$J = E\left\{\left(\frac{\partial}{\partial\theta}\ln f_\theta(x)\right)^2\right\}, \tag{1.14}$$

where $f_\theta(x)$ is the probability density function of the observed data $x$ given the unknown parameter $\theta$. The parameter estimator is bounded as follows:

$$E[(\hat{\Theta}-\theta)^2] \geq J^{-1}. \tag{1.15}$$

Equation (1.15) states that the mean square error is always bigger than the Cramer Rao bound, so the Cramer Rao bound is a good way to check the efficiency of the estimator. When the mean square error is closer to the Cramer Rao bound, the estimate of the symbol timing delay is more efficient. Two different Cramer Rao bounds are derived in this thesis: the conditional Cramer Rao bound and the Modified Cramer Rao bound.

# Chapter 2

# BLOCK PROCESSING

## 2.1 Maximum Likelihood Timing Estimators

### 2.1.1 Maximum Likelihood Timing Estimator for Data-aided and Known Channel System

The Maximum Likelihood (ML) estimate of the symbol timing delay $\tau$ is the value of $\tau$ that maximizes the conditional probability density function $p\left(\mathbf{r} \mid \tau, \mathbf{H}, \mathbf{A}\right)$ based on an observation of $\mathbf{r}(t)$ over an interval of $T_0 = LT_s$ seconds. The solution to this problem is well known for the single-input, single output (SISO) case [10] and the analysis in this thesis follows the standard procedure. The conditional probability density function of the $m$-th element in the vector $\mathbf{r}(t)$ is

$$p\left(r_m \mid \tau, \mathbf{H}, \mathbf{A}\right) = C \exp\left\{ -\frac{1}{N_0} \int_{T_0} \left| r_m(t) - \sum_{i=1}^{N_T} h_{m,i} s_i(t-\tau) \right|^2 dt \right\}. \tag{2.1}$$

Expanding the integral and noting that $\int_{T_0} \left|r_m(t)\right|^2 dt$ does not depend on $\tau$, the conditional density function of $r_m(t)$ can be expressed as

$$\begin{aligned} &p\left(r_m \mid \tau, \mathbf{H}, \mathbf{A}\right) \\ &= C \exp\left\{ \frac{2}{N_0} \int_{T_0} \mathrm{Re}\{r_m(t) \sum_{i=1}^{N_T} h_{m,i}^* s_i^*(t-\tau)\} dt - \frac{1}{N_0} \int_{T_0} \left| \sum_{i=1}^{N_T} h_{m,i} s_i(t-\tau) \right|^2 dt \right\} \end{aligned} \tag{2.2}$$

where the terms that do not depend on $\tau$ have been absorbed into the constant $C$. Assuming spatially white additive noise, the joint probability density function of $\mathbf{r}(t)$

is the product of the density functions of the $r_m(t)$ so that

$$\begin{aligned} p\left(\mathbf{r} \mid \tau, \mathbf{H}, \mathbf{A}\right) =& C^{N_R} \exp\left\{ \frac{2}{N_0} \int_{T_0} \sum_{m=1}^{N_R} Re\{r_m(t) \sum_{i=1}^{N_T} h_{m,i}^* s_i^*(t-\tau)\} dt \right. \\ & \left. - \frac{1}{N_0} \int_{T_0} \sum_{m=1}^{N_R} \left| \sum_{i=1}^{N_T} h_{m,i} s_i(t-\tau) \right|^2 dt \right\}. \end{aligned} \tag{2.3}$$

The log-likelihood function is the logarithm of the conditional probability density function and can be expressed as

$$\begin{aligned} \Lambda\left(\tau; \mathbf{H}, \mathbf{A}\right) =& N_R \ln C + \frac{2}{N_0} \int_{T_0} \sum_{m=1}^{N_R} Re\{r_m(t) \sum_{i=1}^{N_T} h_{m,i} s_i(t-\tau)\} dt \\ & - \frac{1}{N_0} \int_{T_0} \sum_{m=1}^{N_R} \left| \sum_{i=1}^{N_T} h_{m,i} s_i(t-\tau) \right|^2 dt. \end{aligned} \tag{2.4}$$

When this is expanded, it becomes

$$\begin{aligned} & \Lambda\left(\tau; \mathbf{H}, \mathbf{A}\right) \\ & = N_R \ln C + \frac{2}{N_0} \int_{T_0} \sum_{m=1}^{N_R} Re\{r_m(t) \sum_{i=1}^{N_T} h_{m,i}^* s_i^*(t-\tau)\} dt \\ & - \frac{1}{N_0} \int_{T_0} \sum_{m=1}^{N_R} \sum_{i=1}^{N_T} h_{m,i} s_i(t-\tau) \sum_{i'=1}^{N_T} h_{m,i'}^* s_i'^*(t-\tau) dt \\ & = N_R \ln C + \frac{2}{N_0} \sum_{m=1}^{N_R} Re\left\{ \sum_{i=1}^{N_T} h_{mi}^* \sum_{k=-L_p}^{L_0+L_p-1} a_i(k)^* \int_{T_0} r_m(t) p'(t - kT_s - \tau) dt \right\} \\ & - \frac{1}{N_0} \sum_{m=1}^{N_R} \sum_{i=1}^{N_T} h_{mi} \sum_{k=-L_p}^{L_0+L_p-1} a_i(k) \sum_{i'=1}^{N_T} h_{mi'}^* \sum_{k'=-L_p}^{L_0+L_p-1} a_{i'}(k')^* \\ & \times \int_{T_0} p(t - kT_s - \tau) p(t - k'T_s - \tau) dt. \end{aligned} \tag{2.5}$$

The matched filter output matrix $\mathbf{X}(\tau)$ is formed by placing the matched filter outputs from each receive antenna into rows:

$$\mathbf{X}(\tau) = \begin{bmatrix} x_1(-L_pT_s + \tau) & \cdots & x_1((L_0 + L_p - 1)T_s + \tau) \\ x_2(-L_pT_s + \tau) & \cdots & x_2((L_0 + L_p - 1)T_s + \tau) \\ \vdots & \cdots & \vdots \\ x_{N_R}(-L_pT_s + \tau) & \cdots & x_{N_R}((L_0 + L_p - 1)T_s + \tau) \end{bmatrix}, \tag{2.6}$$

where

$$x_m\left(kT_s+\tau\right)=\int_{T_0} r_m(t)p\left(t-kT_s-\tau\right)dt. \tag{2.7}$$

Using the matrix definitions (1.5), (1.8), (1.10) and (2.6), the compact matrix form for (2.5) is given by

$$\Lambda\left(\tau;\mathbf{H},\mathbf{A}\right)=-\frac{2}{N_0}\mathrm{Re}\left\{\mathrm{trace}\left\{\mathbf{HAX}^{\mathcal{H}}(\tau)\right\}\right\}+\frac{1}{N_0}\mathrm{trace}\left\{\mathbf{HAR}(\tau)\mathbf{A}^{\mathcal{H}}\mathbf{H}^{\mathcal{H}}\right\}, \tag{2.8}$$

where

$$\mathbf{R}(\tau)=\int_{T_0}\mathbf{P}(t;\tau)\mathbf{P}^{\mathcal{H}}(t;\tau)dt. \tag{2.9}$$

Then the maximum likelihood estimator for the symbol timing delay is expressed as

$$\begin{aligned}\tau_{ML}&=\underset{\tau}{\mathrm{argmax}}\left\{\Lambda(\tau;\mathbf{H},\mathbf{A})\right\}\\&=\underset{\tau}{\mathrm{argmax}}\left\{-\frac{2}{N_0}\mathrm{Re}\left\{\mathrm{trace}\left\{\mathbf{HAX}^{\mathcal{H}}(\tau)\right\}\right\}+\frac{1}{N_0}\mathrm{trace}\left\{\mathbf{HAR}(\tau)\mathbf{A}^{\mathcal{H}}\mathbf{H}^{\mathcal{H}}\right\}\right\}.\end{aligned} \tag{2.10}$$

Note that when $L_0$, the length of the data sequence, is large enough to make

$$\int_{T_0}\mathbf{P}(t;\tau)\mathbf{P}^{\mathcal{H}}(t;\tau)dt\approx\mathbf{I}, \tag{2.11}$$

the last term in the argument of (2.10) may be omitted so that the Maximum Likelihood timing estimate may be expressed as

$$\tau_{ML}=\arg\max\left\{\mathrm{Re}\left\{\mathrm{trace}\left\{\mathbf{HAX}^{\mathcal{H}}(\tau)\right\}\right\}\right\}. \tag{2.12}$$

The maximum likelihood estimator of the symbol timing delay can also be found without using the previous approximation. Computing the derivative of (2.8) with respect to $\tau$ and setting it equal to zero produces the following necessary condition for (2.10):

$$\frac{\partial}{\partial\tau}\Lambda\left(\tau_{ML};\mathbf{H},\mathbf{A}\right)=0. \tag{2.13}$$

The partial derivative of the log-likelihood function with respect to $\tau$ is

$$\begin{aligned}\frac{\partial}{\partial\tau}\Lambda\left(\tau;\mathbf{H},\mathbf{A}\right) &= -\frac{2}{N_0}Re\left\{\sum_{m=1}^{N_R}\sum_{i=1}^{N_T}h_{m,i}^{*}\sum_{k=-L_p}^{L_0+L_p-1}a_i(k)^{*}x_m(t-kT-\tau)\right\}\\ &+\frac{1}{N_0}\sum_{m=1}^{N_R}\sum_{i=1}^{N_T}h_{mi}\sum_{k=-L_p}^{L_0+L_p-1}a_i(k)\sum_{i'=1}^{N_T}h_{mi'}^{*}\sum_{k'=-L_p}^{L_0+L_p-1}a_{i'}(k')^{*}\\ &\times\int_{T_0}p'(t-kT_s-\tau)p(t-k'T_s-\tau)dt\\ &+\frac{1}{N_0}\sum_{m=1}^{N_R}\sum_{i=1}^{N_T}h_{mi}\sum_{k=-L_p}^{L_0+L_p-1}a_i(k)\sum_{i'=1}^{N_T}h_{mi'}^{*}\sum_{k'=-L_p}^{L_0+L_p-1}a_{i'}(k')^{*}\\ &\times\int_{T_0}p(t-kT_s-\tau)p'(t-k'T_s-\tau)dt,\end{aligned}\tag{2.14}$$

where

$$x'_m(kT+\tau)=\frac{\partial}{\partial\tau}x_m(kT_s+\tau).\tag{2.15}$$

Equation (2.15) can be expressed as

$$x'_m\left(kT_s+\tau\right)=\int_{T_0}r_m(t)p'\left(t-kT_s-\tau\right)dt\tag{2.16}$$

where $p'(t)$ is the time derivative of the common pulse shape $p(t)$. Using the matrix definitions (1.5), (1.8), (2.6) and (1.10) together with

$$\mathbf{X}'(\tau)=\begin{bmatrix}x'_1(-L_pT_s+\tau) & \cdots & x'_1((L_0+L_p-1)T_s+\tau)\\ x'_2(-L_pT_s+\tau) & \cdots & x'_2((L_0+L_p-1)T_s+\tau)\\ \vdots & \cdots & \vdots\\ x'_{N_R}(-L_pT_s+\tau) & \cdots & x'_{N_R}((L_0+L_p-1)T_s+\tau)\end{bmatrix},\tag{2.17}$$

$$\mathbf{P}'(\tau)=\begin{bmatrix}p'(t-T_s-\tau)\\ p'(t-2T_s-\tau)\\ \vdots\\ p'(t-LT_s-\tau)\end{bmatrix},\tag{2.18}$$

equation (2.14) can be expressed in the compact form

$$\begin{aligned}\frac{\partial}{\partial\tau}\Lambda\left(\tau;\mathbf{H},\mathbf{A}\right) =& -\frac{2}{N_0}Re\left\{\text{trace}\left\{\mathbf{HAX}'^{\mathcal{H}}(\tau)\right\}\right\} \\ &+\frac{2}{N_0}Re\left\{\text{trace}\left\{\mathbf{HA}\left(\int_{T_0}\mathbf{P}'(t;\tau)\mathbf{P}^{\mathcal{H}}(t;\tau)dt\right)\mathbf{A}^{\mathcal{H}}\mathbf{H}^{\mathcal{H}}\right\}\right\} \\ =& -\frac{2}{N_0}Re\left\{\text{trace}\left\{\mathbf{HAX}'^{\mathcal{H}}(\tau)\right\}\right\} \\ &+\frac{2}{N_0}Re\left\{\text{trace}\left\{\mathbf{HAR}'(\tau)\mathbf{A}^{\mathcal{H}}\mathbf{H}^{\mathcal{H}}\right\}\right\},\end{aligned} \tag{2.19}$$

where

$$\mathbf{R}'(\tau) = \int_{T_0}\mathbf{P}'(t;\tau)\mathbf{P}^{\mathcal{H}}(t;\tau)dt. \tag{2.20}$$

The maximum likelihood estimator of the symbol timing delay is the value of $\tau$ that make equation (2.19) equal to zero,

$$-\frac{2}{N_0}Re\left\{\text{trace}\left\{\mathbf{HAX}'^{\mathcal{H}}(\tau_{ML})\right\}\right\} + \frac{2}{N_0}Re\left\{\text{trace}\left\{\mathbf{HAR}'(\tau_{ML})\mathbf{A}^{\mathcal{H}}\mathbf{H}^{\mathcal{H}}\right\}\right\} = 0. \tag{2.21}$$

### 2.1.2 Maximum Likelihood Timing Estimator for Data-aided and Unknown Channel System

For the data-aided and unknown channel system, the maximum likelihood estimator of the channel matrix $\mathbf{H}$ is derived and substituted into the log-likelihood equation to get the maximum likelihood estimator for the symbol timing delay $\tau$.

The log-likelihood function was derived from the conditional probability density function in section 2.1.1 to be

$$\Lambda(\tau;\mathbf{H},\mathbf{A}) = -\frac{1}{N_0}\int_{T_0}\left\{\sum_{m=1}^{N_R}\left|r_m(t) - \sum_{i=1}^{N_T}h_{mi}s_i(t,\tau)\right|^2\right\}dt. \tag{2.22}$$

Using the matrix forms (1.5), (1.8), (2.6) and (2.9), the matrix form of (2.22) is

$$\Lambda\left(\tau;\mathbf{H},\mathbf{A}\right) = -\frac{2}{N_0}Re\left\{\text{trace}\left\{\mathbf{HAX}^{\mathcal{H}}(\tau)\right\}\right\} + \frac{1}{N_0}\text{trace}\left\{\mathbf{HAR}(\tau)\mathbf{A}^{\mathcal{H}}\mathbf{H}^{\mathcal{H}}\right\}. \tag{2.23}$$

By taking the partial derivative of (2.23) with respect to the channel matrix $\mathbf{H}$, the maximum likelihood estimator of the channel gain is found. The maximum likelihood

estimator of the channel gain is

$$\mathbf{H}_{ML} = \mathbf{X}(\tau)\mathbf{A}^{\mathcal{H}}[\mathbf{A}\mathbf{A}^{\mathcal{H}}]^{-1}. \tag{2.24}$$

The log-likelihood function used to find the maximum likelihood estimator of the timing delay $\tau$ is

$$\Lambda\left(\tau; \mathbf{H}_{ML}, \mathbf{A}\right) = -\frac{2}{N_0} Re\left\{\text{trace}\left\{\mathbf{H}_{ML}\mathbf{A}\mathbf{X}^{\mathcal{H}}(\tau)\right\}\right\} + \frac{1}{N_0}\text{trace}\left\{\mathbf{H}_{ML}\mathbf{A}\mathbf{R}(\tau)\mathbf{A}^{\mathcal{H}}\mathbf{H}_{ML}^{\mathcal{H}}\right\}. \tag{2.25}$$

Replacing the unknown channel matrix with the maximum likelihood estimator for the channel matrix, the log-likelihood function becomes

$$\begin{aligned}\Lambda(\tau; \mathbf{H}_{ML}, \mathbf{A}) = &-\frac{2}{N_0}\text{Re}\left\{\text{trace}\left\{\mathbf{X}(\tau)\mathbf{A}^{\mathcal{H}}(\mathbf{A}\mathbf{A}^{\mathcal{H}})^{-1}\mathbf{A}\mathbf{X}^{\mathcal{H}}(\tau)\right\}\right\} \\ &+ \frac{1}{N_0}\text{trace}\left\{\mathbf{X}(\tau)\mathbf{A}^{\mathcal{H}}(\mathbf{A}\mathbf{A}^{\mathcal{H}})^{-1}\mathbf{A}\mathbf{R}(\tau)\mathbf{A}^{\mathcal{H}}(\mathbf{A}\mathbf{A}^{\mathcal{H}})^{-1}\mathbf{A}\mathbf{X}^{\mathcal{H}}(\tau)\right\}.\end{aligned} \tag{2.26}$$

The maximum likelihood estimator for the symbol timing delay is

$$\begin{aligned}\tau_{ML} &= \underset{\tau}{\text{argmax}}\left\{\Lambda(\tau; \mathbf{H}_{ML}, \mathbf{A})\right\} \\ &= \underset{\tau}{\text{argmax}}\left\{-\frac{2}{N_0}\text{Re}\left\{\text{trace}\left\{\mathbf{X}(\tau)\mathbf{A}^{\mathcal{H}}(\mathbf{A}\mathbf{A}^{\mathcal{H}})^{-1}\mathbf{A}\mathbf{X}^{\mathcal{H}}(\tau)\right\}\right\}\right. \\ &\left.+\frac{1}{N_0}\text{trace}\{\mathbf{X}(\tau)\mathbf{A}^{\mathcal{H}}(\mathbf{A}\mathbf{A}^{\mathcal{H}})^{-1}\mathbf{A}\mathbf{R}(\tau)\mathbf{A}^{\mathcal{H}}(\mathbf{A}\mathbf{A}^{\mathcal{H}})^{-1}\mathbf{A}\mathbf{X}^{\mathcal{H}}(\tau)\}\right\}.\end{aligned} \tag{2.27}$$

When $L_0$ is large enough, $\mathbf{R}(\tau) = \int_{T_0}\mathbf{P}(t;\tau)\mathbf{P}^{\mathcal{H}}(t;\tau)dt \approx \mathbf{I}$. If the $N_T$ training sequences represented by $\mathbf{A}$ are orthogonal, then $\mathbf{A}\mathbf{A}^{\mathcal{H}} = \mathbf{I}$. The matrix $\mathbf{B}$ is defined as $\mathbf{B} = \mathbf{A}^{\mathcal{H}}\mathbf{A}$, the outer product of the data sequences. Using the approximation for $\mathbf{R}(\tau)$, the log likelihood function may be expressed in the form

$$\begin{aligned}\Lambda(\tau; \mathbf{H}_{ML}, \mathbf{A}) &= -\frac{1}{N_0}\text{Re}\left\{\text{trace}\left\{\mathbf{X}(\tau)\mathbf{A}^{\mathcal{H}}\mathbf{A}\mathbf{X}^{\mathcal{H}}(\tau)\right\}\right\} \\ &= -\frac{1}{N_0}\text{Re}\left\{\text{trace}\left\{\mathbf{X}(\tau)\mathbf{B}\mathbf{X}^{\mathcal{H}}(\tau)\right\}\right\},\end{aligned} \tag{2.28}$$

and the maximum likelihood estimator of the symbol timing delay becomes

$$\begin{aligned}\tau_{ML} &= \underset{\tau}{\text{argmax}}\left\{\Lambda(\tau; \mathbf{H}_{ML}, \mathbf{A})\right\} \\ &= \underset{\tau}{\text{argmax}}\left\{-\frac{1}{N_0}\text{Re}\left\{\text{trace}\left\{\mathbf{X}(\tau)\mathbf{B}\mathbf{X}^{\mathcal{H}}(\tau)\right\}\right\}\right\}.\end{aligned} \tag{2.29}$$

The maximum likelihood estimator of the symbol timing delay can also be found without using the previous approximation. Computing the derivative of (2.23) with respect to $\tau$ and setting it equal to zero produces the necessary condition for (2.29):

$$\frac{\partial}{\partial\tau}\Lambda\left(\tau;\mathbf{H},\mathbf{A}\right)=-\frac{2}{N_0}Re\left\{\text{trace}\left\{\mathbf{H}\mathbf{A}\mathbf{X}'^{\mathcal{H}}(\tau)\right\}\right\}+\frac{2}{N_0}\text{trace}\left\{\mathbf{H}\mathbf{A}\mathbf{R}'(\tau)\mathbf{A}^{\mathcal{H}}\mathbf{H}^{\mathcal{H}}\right\}, \tag{2.30}$$

where $\mathbf{X}'(\tau)$ is defined in (2.17) and $\mathbf{R}'(\tau)$ is defined in (2.20). Substituting $\mathbf{H}_{ML}$ into equation (2.30) produces ,

$$\begin{aligned}\frac{\partial}{\partial\tau}\Lambda\left(\tau;\mathbf{H}_{ML},\mathbf{A}\right)=&-\frac{2}{N_0}Re\left\{\text{trace}\left\{\mathbf{H}_{ML}\mathbf{A}\mathbf{X}'^{\mathcal{H}}(\tau)\right\}\right\}\\&+\frac{2}{N_0}\text{trace}\left\{\mathbf{H}_{ML}\mathbf{A}\mathbf{R}'(\tau)\mathbf{A}^{\mathcal{H}}\mathbf{H}_{ML}^{\mathcal{H}}\right\}.\end{aligned} \tag{2.31}$$

Substituting the maximum likelihood estimator of $\mathbf{H}$ into equation (2.31) produces

$$\begin{aligned}\frac{\partial}{\partial\tau}\Lambda(\tau;\mathbf{H}_{ML},\mathbf{A})=&-\frac{2}{N_0}\text{Re}\left\{\text{trace}\left\{\mathbf{X}'(\tau)\mathbf{A}^{\mathcal{H}}(\mathbf{A}\mathbf{A}^{\mathcal{H}})^{-1}\mathbf{A}\mathbf{X}^{\mathcal{H}}(\tau)\right\}\right\}\\&+\frac{2}{N_0}\text{trace}\left\{\mathbf{X}(\tau)\mathbf{A}^{\mathcal{H}}(\mathbf{A}\mathbf{A}^{\mathcal{H}})^{-1}\mathbf{A}\mathbf{R}'(\tau)\mathbf{A}^{\mathcal{H}}(\mathbf{A}\mathbf{A}^{\mathcal{H}})^{-1}\mathbf{A}\mathbf{X}^{\mathcal{H}}(\tau)\right\}.\end{aligned} \tag{2.32}$$

The data-aided unknown channel maximum likelihood estimator of the symbol timing delay is the value of $\tau$ which forces (2.32) to zero,

$$\begin{aligned}0=&-\frac{2}{N_0}\text{Re}\left\{\text{trace}\left\{\mathbf{X}'(\tau_{ML})\mathbf{A}^{\mathcal{H}}(\mathbf{A}\mathbf{A}^{\mathcal{H}})^{-1}\mathbf{A}\mathbf{X}^{\mathcal{H}}(\tau_{ML})\right\}\right\}\\&+\frac{2}{N_0}\text{trace}\left\{\mathbf{X}(\tau_{ML})\mathbf{A}^{\mathcal{H}}(\mathbf{A}\mathbf{A}^{\mathcal{H}})^{-1}\mathbf{A}\mathbf{R}'(\tau_{ML})\mathbf{A}^{\mathcal{H}}(\mathbf{A}\mathbf{A}^{\mathcal{H}})^{-1}\mathbf{A}\mathbf{X}^{\mathcal{H}}(\tau_{ML})\right\}.\end{aligned} \tag{2.33}$$

### 2.1.3 Maximum Likelihood Timing Estimator for Non-data-aided and Known Channel System

For the non-data-aided and known channel system, first the maximum likelihood estimator for the data matrix $\mathbf{A}$ is derived. Then the unknown data matrix is replaced with the maximum likelihood estimator of the unknown data matrix, $\mathbf{A}_{ML}$, in the log-likelihood equation to get the maximum likelihood estimator of the symbol timing delay $\tau$.

The log-likelihood function was derived from the conditional probability density function in section 2.1.1 to be

$$\Lambda(\tau;\mathbf{H},\mathbf{A}) = -\frac{1}{N_0}\int_{T_0}\left\{\sum_{m=1}^{N_R}\left|r_m(t)-\sum_{i=1}^{N_T}h_{mi}s_i(t,\tau)\right|^2\right\}dt. \tag{2.34}$$

Using the matrix forms (1.5), (1.8), (2.6) and (2.9), the matrix form of (2.34) is

$$\Lambda\left(\tau;\mathbf{H},\mathbf{A}\right) = -\frac{2}{N_0}Re\left\{\text{trace}\left\{\mathbf{H}\mathbf{A}\mathbf{X}^{\mathcal{H}}(\tau)\right\}\right\} + \frac{1}{N_0}\text{trace}\left\{\mathbf{H}\mathbf{A}\mathbf{R}(\tau)\mathbf{A}^{\mathcal{H}}\mathbf{H}^{\mathcal{H}}\right\}. \tag{2.35}$$

By taking the partial derivative of (2.35) with respect to the data matrix $\mathbf{A}$, the maximum likelihood estimator of the data matrix is found:

$$\mathbf{A}_{ML} = (\mathbf{H}^{\mathcal{H}}\mathbf{H})^{-1}\mathbf{H}^{\mathcal{H}}\mathbf{X}(\tau). \tag{2.36}$$

The log-likelihood function for the non-data-aided and known channel system is

$$\Lambda\left(\tau;\mathbf{H},\mathbf{A}_{ML}\right) = -\frac{2}{N_0}Re\left\{\text{trace}\left\{\mathbf{H}\mathbf{A}_{ML}\mathbf{X}^{\mathcal{H}}(\tau)\right\}\right\} + \frac{1}{N_0}\text{trace}\left\{\mathbf{H}\mathbf{A}_{ML}\mathbf{R}(\tau)\mathbf{A}_{ML}^{\mathcal{H}}\mathbf{H}^{\mathcal{H}}\right\}. \tag{2.37}$$

Replacing the unknown data matrix with the maximum likelihood estimator of the data matrix, the log-likelihood function becomes

$$\begin{aligned}\Lambda\left(\tau;\mathbf{H},\mathbf{A}_{ML}\right) &= -\frac{2}{N_0}Re\left\{\text{trace}\left\{\mathbf{H}(\mathbf{H}^{\mathcal{H}}\mathbf{H})^{-1}\mathbf{H}^{\mathcal{H}}\mathbf{X}(\tau)\mathbf{X}^{\mathcal{H}}(\tau)\right\}\right\}\\ &+\frac{1}{N_0}\text{trace}\left\{\mathbf{H}(\mathbf{H}^{\mathcal{H}}\mathbf{H})^{-1}\mathbf{H}^{\mathcal{H}}\mathbf{X}(\tau)\mathbf{R}(\tau)\mathbf{X}(\tau)^{\mathcal{H}}\mathbf{H}(\mathbf{H}^{\mathcal{H}}\mathbf{H})^{-1}\mathbf{H}^{\mathcal{H}}\right\}.\end{aligned} \tag{2.38}$$

The maximum likelihood estimator of the symbol timing delay $\tau$ is

$$\begin{aligned}\tau_{ML} &= \underset{\tau}{\text{argmax}}\left\{\Lambda(\tau;\mathbf{H},\mathbf{A}_{ML})\right\}\\ &= \underset{\tau}{\text{argmax}}\left\{-\frac{2}{N_0}Re\left\{\text{trace}\left\{\mathbf{H}(\mathbf{H}^{\mathcal{H}}\mathbf{H})^{-1}\mathbf{H}^{\mathcal{H}}\mathbf{X}(\tau)\mathbf{X}^{\mathcal{H}}(\tau)\right\}\right\}\right.\\ &\left.+\frac{1}{N_0}\text{trace}\left\{\mathbf{H}(\mathbf{H}^{\mathcal{H}}\mathbf{H})^{-1}\mathbf{H}^{\mathcal{H}}\mathbf{X}(\tau)\mathbf{R}(\tau)\mathbf{X}(\tau)^{\mathcal{H}}\mathbf{H}(\mathbf{H}^{\mathcal{H}}\mathbf{H})^{-1}\mathbf{H}^{\mathcal{H}}\right\}\right\}.\end{aligned} \tag{2.39}$$

Computing the derivative of (2.38) with respect to $\tau$ and setting it equal to zero produces the necessary condition for (2.39).

$$\frac{\partial}{\partial\tau}\Lambda\left(\tau;\mathbf{H},\mathbf{A}\right) = -\frac{2}{N_0}Re\left\{\text{trace}\left\{\mathbf{H}\mathbf{A}\mathbf{X}'^{\mathcal{H}}(\tau)\right\}\right\} + \frac{2}{N_0}\text{trace}\left\{\mathbf{H}\mathbf{A}\mathbf{R}'(\tau)\mathbf{A}^{\mathcal{H}}\mathbf{H}^{\mathcal{H}}\right\}, \tag{2.40}$$

where $\mathbf{X}'(\tau)$ is defined in (2.17) and $\mathbf{R}'(\tau)$ is defined in (2.20). Substituting $\mathbf{A}_{ML}$ into equation (2.40) produces ,

$$\begin{aligned}\frac{\partial}{\partial\tau}\Lambda\left(\tau;\mathbf{H},\mathbf{A}_{ML}\right) = &-\frac{2}{N_0}Re\left\{\text{trace}\left\{\mathbf{H}\mathbf{A}_{ML}\mathbf{X}'^{\mathcal{H}}(\tau)\right\}\right\} \\ &+\frac{2}{N_0}\text{trace}\left\{\mathbf{H}\mathbf{A}_{ML}\mathbf{R}'(\tau)\mathbf{A}_{ML}^{\mathcal{H}}\mathbf{H}^{\mathcal{H}}\right\}.\end{aligned} \tag{2.41}$$

Substituting the maximum likelihood estimator of $\mathbf{A}$ into equation (2.41) produces:

$$\begin{aligned}&\frac{\partial}{\partial\tau}\Lambda\left(\tau;\mathbf{H},\mathbf{A}_{ML}\right) = -\frac{2}{N_0}Re\left\{\text{trace}\left\{\mathbf{H}(\mathbf{H}^{\mathcal{H}}\mathbf{H})^{-1}\mathbf{H}^{\mathcal{H}}\mathbf{X}(\tau)\mathbf{X}'^{\mathcal{H}}(\tau)\right\}\right\} \\ &+\frac{2}{N_0}\text{trace}\left\{\mathbf{H}(\mathbf{H}^{\mathcal{H}}\mathbf{H})^{-1}\mathbf{H}^{\mathcal{H}}\mathbf{X}(\tau)\mathbf{R}'(\tau)\mathbf{X}(\tau)^{\mathcal{H}}\mathbf{H}(\mathbf{H}^{\mathcal{H}}\mathbf{H})^{-1}\mathbf{H}^{\mathcal{H}}\right\}.\end{aligned} \tag{2.42}$$

The non-data-aided and known channel-gain maximum likelihood estimator of the symbol timing delay is the value of $\tau$ which forces equation (2.42) to zero,

$$\begin{aligned}0 = &-\frac{2}{N_0}Re\left\{\text{trace}\left\{\mathbf{H}(\mathbf{H}^{\mathcal{H}}\mathbf{H})^{-1}\mathbf{H}^{\mathcal{H}}\mathbf{X}(\tau)\mathbf{X}'^{\mathcal{H}}(\tau)\right\}\right\} \\ &+\frac{2}{N_0}\text{trace}\left\{\mathbf{H}(\mathbf{H}^{\mathcal{H}}\mathbf{H})^{-1}\mathbf{H}^{\mathcal{H}}\mathbf{X}(\tau)\mathbf{R}'(\tau)\mathbf{X}(\tau)^{\mathcal{H}}\mathbf{H}(\mathbf{H}^{\mathcal{H}}\mathbf{H})^{-1}\mathbf{H}^{\mathcal{H}}\right\}.\end{aligned} \tag{2.43}$$

### 2.1.4 Maximum Likelihood Timing Estimator for Non-data-aided and Unknown Channel System

For the non-data-aided and unknown channel system, timing estimation is more complex than in the other three cases. Without knowledge of the data transmitted, the channel of the MIMO system is hard to estimate.

One way to estimate the symbol timing delay for the non-data-aided and unknown channel system is introduced in [13]. Instead of using the training sequence to estimate the channel matrix, the channel matrix and the data matrix are combined into one variable. For the system model defined as

$$\mathbf{r}(t) = \mathbf{HAP}(t;\tau) + \mathbf{w}(t), \tag{2.44}$$

$\mathbf{HA}$ can be treated as a new matrix $\mathbf{Z}$. Then the system model can be expressed as

$$\mathbf{r}(t) = \mathbf{ZP}(t;\tau) + \mathbf{w}(t). \tag{2.45}$$

The data matrix and the channel matrix are unknown, so the new matrix $\mathbf{Z}$ is also unknown. Changing two unknown matrices into one unknown matrix makes the

timing delay estimate easier to calculate because the channel and data matrices no longer have to be estimated separately.

The log-likelihood function is

$$\Lambda\left(\tau;\mathbf{H},\mathbf{A}\right)=-\frac{2}{N_0}Re\left\{\text{trace}\left\{\mathbf{HAX}^{\mathcal{H}}(\tau)\right\}\right\}+\frac{1}{N_0}\text{trace}\left\{\mathbf{HAR}(\tau)\mathbf{A}^{\mathcal{H}}\mathbf{H}^{\mathcal{H}}\right\}. \quad (2.46)$$

Then the log-likelihood function using $\mathbf{Z}$ is expressed as

$$\Lambda\left(\tau;\mathbf{Z}\right)=-\frac{2}{N_0}Re\left\{\text{trace}\left\{\mathbf{ZX}^{\mathcal{H}}(\tau)\right\}\right\}+\frac{1}{N_0}\text{trace}\left\{\mathbf{ZR}(\tau)\mathbf{Z}^{\mathcal{H}}\right\}. \quad (2.47)$$

First, the maximum likelihood estimator of the unknown matrix $\mathbf{Z}$ is obtained by taking the derivative of (2.47) with respect to $\mathbf{Z}$,

$$\frac{\partial}{\partial\mathbf{Z}}\Lambda(\tau;\mathbf{Z})=-\frac{2}{N_0}Re\left\{\mathbf{X}^{*}(\tau)\right\}+\frac{2}{N_0}\mathbf{R}^{*}(\tau)\mathbf{Z}^{*}. \quad (2.48)$$

Then (2.48) is set equal to zero:

$$-\mathbf{X}(\tau)+\mathbf{ZR}(\tau)=0. \quad (2.49)$$

The maximum likelihood estimator for $\mathbf{Z}$ is the value of $\mathbf{Z}$ that makes equation(2.49) true:

$$\mathbf{Z}_{ML}=\mathbf{X}(\tau)\left(\mathbf{R}(\tau)\right)^{-1}. \quad (2.50)$$

Next the maximum likelihood estimator of $\mathbf{Z}$ is substituted into the log-likelihood function. The resulting log-likelihood function is

$$\Lambda\left(\tau;\mathbf{Z}_{ML}\right)=\frac{1}{N_0}Re\left\{\text{trace}\left\{\mathbf{X}(\tau)\mathbf{R}(\tau)^{-1}\mathbf{X}^{\mathcal{H}}(\tau)\right\}\right\}. \quad (2.51)$$

Then the maximum likelihood estimator for the symbol timing delay is

$$\begin{aligned}\tau_{ML}&=\underset{\tau}{\text{argmax}}\Lambda(\tau;\mathbf{Z})\\&=\underset{\tau}{\text{argmax}}\left\{\frac{1}{N_0}Re\left\{\text{trace}\left\{\mathbf{X}(\tau)\mathbf{R}(\tau)^{-1}\mathbf{X}^{\mathcal{H}}(\tau)\right\}\right\}\right\}\end{aligned} \quad (2.52)$$

When $L_0$ is large enough to make $\mathbf{R}(\tau)=\mathbf{I}$, the estimator (2.52) reduces to

$$\tau_{ML}=\underset{\tau}{\text{argmax}}\left\{\frac{1}{N_0}Re\left\{\text{trace}\left\{\mathbf{X}(\tau)\mathbf{X}^{\mathcal{H}}(\tau)\right\}\right\}\right\}. \quad (2.53)$$

The maximum likelihood estimator for the symbol timing delay can also be found without the previous approximation. Computing the derivative of (2.51) with respect to $\tau$ and setting it equal to zero produces the necessary condition for (2.52):

$$\frac{\partial}{\partial\tau}\Lambda\left(\tau;\mathbf{Z}_{ML}\right)=-\frac{2}{N_0}Re\left\{\text{trace}\left\{\mathbf{Z}_{ML}\mathbf{X}'^{\mathcal{H}}(\tau)\right\}\right\}+\frac{2}{N_0}\text{trace}\left\{\mathbf{Z}_{ML}\mathbf{R}'(\tau)\mathbf{Z}_{ML}^{\mathcal{H}}\right\}. \tag{2.54}$$

The non-data-aided and unknown channel-gain maximum likelihood estimator of the symbol timing delay is the value of $\tau$ which forces equation (2.54) to zero:

$$0=-\frac{2}{N_0}Re\left\{\text{trace}\left\{\mathbf{Z}\mathbf{X}'^{\mathcal{H}}(\tau_{ML})\right\}\right\}+\frac{2}{N_0}\text{trace}\left\{\mathbf{Z}\mathbf{R}'(\tau_{ML})\mathbf{Z}^{\mathcal{H}}\right\}. \tag{2.55}$$

## 2.2 Cramer Rao Bound for the Symbol Timing Estimator

The Cramer Rao bound is the lower bound of the mean-square error of the estimator. The mean square error of the estimator is an important way to measure the accuracy of the estimation. By comparing the mean square error and the Cramer Rao bound, the efficiency of the estimator is measured. The efficiency of the estimator is a measure of how close the mean square error is to the minimum possible. This thesis uses two different Cramer Rao bounds to do this comparison. One is the Modified Cramer Rao bound, and the other is the Conditional Cramer Rao bound.

The Cramer Rao bound is based on the Fisher Information Matrix, which is defined as

$$\begin{aligned}J&=E\left\{\left(\frac{\partial}{\partial\theta}\ln f_\theta(x)\right)^2\right\}\\&=E\left\{\left(\frac{\partial}{\partial\theta}\Lambda(x;\theta)\right)^2\right\}.\end{aligned} \tag{2.56}$$

In equation (2.56), $f_\theta(x)$ is the probability density function of the observed data $x$ given the unknown parameter $\theta$, and $\Lambda(x;\theta)$ is the log-likelihood function of the observed data $x$ given unknown parameter $\theta$. The mean square error of the parameter estimator is bounded as follows:

$$E[(\hat{\Theta}-\theta)^2]\geq J^{-1}. \tag{2.57}$$

### 2.2.1 Modified Cramer Rao Bound

The real application of this for synchronization problems is difficult. There may be more than one unknown parameter in the log-likelihood function. If this is the case, the log-likelihood function given the wanted unknown parameter can be found by averaging out the unwanted parameters from the log-likelihood function $\Lambda(x;\theta,u)$.

$$\Lambda(x;\theta) = \int_{-\infty}^{\infty} \Lambda(x;\theta,u)p(u)du \tag{2.58}$$

The integration in (2.58) can't be performed analytically, because the expectation in (2.56) has insuperable obstacles. As introduced in [10], one method used to overcome these obstacles is called the Modified Cramer Rao Bound (MCRB). The received signal at the $mth$ antenna is

$$r_m(t) = \sum_{i=1}^{N_T} h_{mi} \sum_{k=-L_p}^{L_0+L_p-1} a_i(k)p(t-kT_s-\tau) + w_m(t). \tag{2.59}$$

The variance of the error of the symbol timing delay estimator is higher than the Cramer Rao bound. This can be denoted as

$$E\left\{|\tau-\tau_{ML}|^2\right\} \geq \frac{1}{E\left\{|\frac{\partial}{\partial\tau}\Lambda(\tau)|^2\right\}}. \tag{2.60}$$

The Modified Cramer Rao Bound (MCRB) is given as

$$E\left\{|\tau-\tau_{ML}|^2\right\} \geq \frac{N_0}{E\left\{\int_0^{L_0T_s} |\frac{\partial}{\partial\tau}\sum_{m=1}^{N_R}\sum_{i=1}^{N_T} h_{mi}\sum_{k=-L_p}^{L_0+L_p-1} a_i(k)p(t-kT_s-\tau)|^2dt\right\}}. \tag{2.61}$$

In order to simplify the denominator of equation (2.61), the partial derivative is calculated and the magnitude squared term is expanded. The partial derivative of $\sum_{m=1}^{N_R} s_m(t,\tau)$ with respect to $\tau$ is

$$\begin{aligned} &\frac{\partial}{\partial\tau}\left\{\sum_{m=1}^{N_R}\sum_{i=1}^{N_T} h_{mi}\sum_{k=-L_p}^{L_0+L_p-1} a_i(k)p(t-kT_s-\tau)\right\} \\ &= -\sum_{m=1}^{N_R}\sum_{i=1}^{N_T} h_{mi}\sum_{k=-L_p}^{L_0+L_p-1} a_i(k)p'(t-kT_s-\tau), \end{aligned} \tag{2.62}$$

where $p'(t - kT_s - \tau) = -\frac{\partial}{\partial \tau} p(t - kT_s - \tau)$. The magnitude squared term can be written as

$$\begin{aligned}
&\left| \frac{\partial}{\partial \tau} \sum_{m=1}^{N_R} \sum_{i=1}^{N_T} h_{mi} \sum_{k=-L_p}^{L_0+L_p-1} a_i(k) p(t - kT_s - \tau) \right|^2 \\
&= \left\{ \sum_{m=1}^{N_R} \sum_{i=1}^{N_T} h_{mi} \sum_{k=-L_p}^{L_0+L_p-1} a_i(k) p'(t - kT_s - \tau) \right\} \\
&\times \left\{ \sum_{m=1}^{N_R} \sum_{i=1}^{N_T} h_{mi} \sum_{k=-L_p}^{L_0+L_p-1} a_i(k) p'(t - kT_s - \tau) \right\}^* .
\end{aligned} \tag{2.63}$$

When equation (2.63) is expanded, it becomes:

$$\begin{aligned}
&\left| \frac{\partial}{\partial \tau} \sum_{m=1}^{N_R} \sum_{i=1}^{N_T} h_{mi} \sum_{k=-L_p}^{L_0+L_p-1} a_i(k) p(t - kT_s - \tau) \right|^2 \\
&= \sum_{m=1}^{N_R} \sum_{i=1}^{N_T} h_{mi} \sum_{k=-L_p}^{L_0+L_p-1} a_i(k) \sum_{m'=1}^{N_R} \sum_{i'=1}^{N_T} h^*_{m'i'} \\
&\times \sum_{k'=-L_p}^{L_0+L_p-1} a_{i'}(k')^* p'(t - kT_s - \tau) p'(t - k'T_s - \tau).
\end{aligned} \tag{2.64}$$

The argument of the expectation in the denominator of equation (2.61) can now be written as

$$\begin{aligned}
&\int_0^{L_0 T_s} \left| \frac{\partial}{\partial \tau} \sum_{m=1}^{N_R} \sum_{i=1}^{N_T} h_{mi} \sum_{k=-L_p}^{L_0+L_p-1} a_i(k) p(t - kT_s - \tau) \right|^2 dt \\
&= \sum_{m=1}^{N_R} \sum_{i=1}^{N_T} h_{mi} \sum_{k=-L_p}^{L_0+L_p-1} a_i(k) \sum_{\hat{m}=1}^{N_R} \sum_{i'=1}^{N_T} h^*_{m'i'} \\
&\times \sum_{k'=-L_p}^{L_0+L_p-1} a_{i'}(k')^* \int_0^{L_0 T_s} p'(t - kT_s - \tau) p'(t - k'T_s - \tau) dt.
\end{aligned} \tag{2.65}$$

The denominator of equation (2.61) is the expectation of equation (2.65), which is

$$\begin{aligned}
&E\left\{\int_0^{L_0T_s}\left|\sum_{m=1}^{N_R}\sum_{i=1}^{N_T}h_{mi}\sum_{k=-L_p}^{L_0+L_p-1}a_i(k)p(t-kT_s-\tau)\right|^2 dt\right\}\\
&=\int_0^{L_0T_s}E\left\{\left|\sum_{m=1}^{N_R}\sum_{i=1}^{N_T}h_{mi}\sum_{k=-L_p}^{L_0+L_p-1}a_i(k)p(t-kT_s-\tau)\right|^2\right\}dt\\
&=\int_0^{L_0T_s}E\left\{\sum_{m=1}^{N_R}\sum_{i=1}^{N_T}h_{mi}\sum_{k=-L_p}^{L_0+L_p-1}a_i(k)\sum_{m'=1}^{N_R}\sum_{i'=1}^{N_T}h^*_{m'i'}\right.\\
&\left.\times\sum_{k'=-L_p}^{L_0+L_p-1}a_{i'}(k')^*p'(t-kT_s-\tau)p'(t-k'T_s-\tau)\right\}dt.
\end{aligned}\tag{2.66}$$

According to the definition of the Modified Cramer Rao bound, the expectation should first be calculated over the undesired unknown parameters and then calculated over the estimator. In this derivation, it is assumed that the data is the undesired unknown parameter, and the symbol timing delay, $\tau$, is the estimator. The expectation with respect to the data $\{a_i(j)\}$ can be expressed as

$$\begin{aligned}
&E_a\left\{\left|\sum_{m=1}^{N_R}\sum_{i=1}^{N_T}h_{mi}\sum_{k=-L_p}^{L_0+L_p-1}a_i(k)p(t-kT_s-\tau)\right|^2\right\}\\
&=\sum_{m=1}^{N_R}\sum_{m'=1}^{N_R}E_a\left\{\sum_{i=1}^{N_T}h_{mi}\sum_{i'=1}^{N_T}h^*_{m'i'}\right.\\
&\left.\times\sum_{k=-L_p}^{L_0+L_p-1}\sum_{k'=-L_p}^{L_0+L_p-1}a_i(k)a_{i'}(k')^*p'(t-kT_s-\tau)p'(t-k'T_s-\tau)\right\}.
\end{aligned}\tag{2.67}$$

The data $\{a_{ij}\}$ is assumed to be an independent random variable with

$$E\left\{a_i(j)a_{i'}(j')^*\right\}=\begin{cases}a_2 & \text{if } i=i',j=j'\\ 0 & \text{otherwise}\end{cases},\tag{2.68}$$

so equation (2.67) can be written as

$$E_a \left\{ \left| \sum_{m=1}^{N_R} \sum_{i=1}^{N_T} h_{mi} \sum_{k=-L_p}^{L_0+L_p-1} a_i(k) p(t - kT_s - \tau) \right|^2 \right\} \tag{2.69}$$

$$= \sum_{m=1}^{N_R} \sum_{m'}^{N_R} \sum_{i=1}^{N_T} h_{mi} h^*_{m'i} \sum_{k=-L_p}^{L_0+L_p-1} a_2 p'(t - kT_s - \tau)^2 \tag{2.70}$$

$$= \sum_{m=1}^{N_R} \sum_{m'}^{N_R} \sum_{i=1}^{N_T} h_{mi} h^*_{m'i} a_2 \sum_{k=-L_p}^{L_0+L_p-1} p'(t - kT_s - \tau)^2. \tag{2.71}$$

This is not a good assumption for an space time coding system, but it is used to produce a tractible result.

As described in [10], the Poisson sum formula is

$$\sum_{k=-L_p}^{L_0+L_p-1} p'(t - kT_s - \tau)^2 = \frac{1}{T_s} \sum_{k=-L_p}^{L_0+L_p-1} P_2(\frac{k}{T_s}) \exp\{\frac{j2\pi k(t-\tau)}{T_s}\}, \tag{2.72}$$

where $P_2(f)$ is the Fourier transform of $\int_{-\infty}^{\infty} p'(t)^2$,

$$P_2(f) = \int_{-\infty}^{\infty} P(v) P(f - v) dv \tag{2.73}$$

and $P(v)$ is the Fourier transform of $p'(t)$. Using the Poisson formula, the denominator of equation (2.61) becomes

$$\int_0^{L_0 T_s} E_{a,\tau} \left\{ \left| \sum_{m=1}^{N_R} \sum_{i=1}^{N_T} h_{mi} \sum_{k=-L_p}^{L_0+L_p-1} a_i(k) p(t - kT_s - \tau) \right|^2 \right\} dt \tag{2.74}$$

$$= \sum_{m=1}^{N_R} \sum_{m'}^{N_R} \sum_{i=1}^{N_T} h_{mi} h^*_{m'i} a_2 P_2(0) L_0. \tag{2.75}$$

The average signal energy per symbol is given by

$$E_s = \frac{a_2}{2} \int_{-\infty}^{\infty} |G(f)|^2 \, df. \tag{2.76}$$

Using the fact that $P(v)$ is the Fourier transform of $p'(t)$, equation (2.73) evaluated at zero is

$$P_2(0) = \int_{-\infty}^{\infty} \left\{ \frac{\partial}{\partial t} p(t) \right\}^2 dt \tag{2.77}$$

$$= 4\pi^2 \int_{-\infty}^{\infty} f^2 |G(f)|^2 df, \tag{2.78}$$

where $G(f)$ is the Fourier transform of $p(t)$. The dimensional parameter $\xi$ can be defined as:

$$\xi = T_s^2 \frac{\int_{-\infty}^{\infty} f^2 |G(f)|^2 df}{\int_{-\infty}^{\infty} |G(f)|^2 df}. \tag{2.79}$$

Then the denominator of equation (2.61) becomes:

$$\int_0^{L_0 T_s} E_{a,\tau} \left\{ \left| \sum_{m=1}^{N_R} \sum_{i=1}^{N_T} h_{mi} \sum_{k=-L_p}^{L_0+L_p-1} a_i(k) p(t - kT_s - \tau) \right|^2 \right\} dt \tag{2.80}$$

$$= \sum_{m=1}^{N_R} \sum_{m'=1}^{N_R} \sum_{i=1}^{N_T} h_{mi} h_{m'i}^* \frac{2E_s}{\int_{-\infty}^{\infty} |G(f)|^2 df} 4\pi^2 \int_{-\infty}^{\infty} f^2 |G(f)|^2 df L_0 \tag{2.81}$$

$$= \sum_{m=1}^{N_R} \sum_{m'=1}^{N_R} \sum_{i=1}^{N_T} h_{mi} h_{m'i}^* \frac{8\pi^2 E_s L_0}{T_s^2} \xi. \tag{2.82}$$

If $p(t)$ is a root-raised-cosine function, then the value of $\xi$ is given by

$$\xi = \frac{1}{12} + \alpha^2 (\frac{1}{4} - \frac{2}{\pi^2}) \tag{2.83}$$

[10]. Finally, the Modified Cramer Rao bound for the symbol timing delay estimator is

$$\textbf{MCRB} = \frac{N_0}{\int_0^{L_0 T_s} E_{a,\tau} \left\{ \left| \sum_{m=1}^{N_R} \sum_{i=1}^{N_T} h_{mi} \sum_{k=-L_p}^{L_0+L_p-1} a_i(k) p(t - kT_s - \tau) \right|^2 \right\} dt} \tag{2.84}$$

$$= \frac{T_s^2}{\sum_{m=1}^{N_R} \sum_{m'=1}^{N_R} \sum_{i=1}^{N_T} h_{mi} h_{m'i}^* \frac{8\pi^2 E_s L_0}{N_0} \xi}. \tag{2.85}$$

### 2.2.2 Conditional Cramer Rao Bound

As introduced in [13], the conditional Cramer Rao bound is derived from the conditional maximum likelihood estimator. Instead of averaging out the undesired parameters, they are written as a function of the desired parameter and the signal. This is called conditional maximum likelihood estimation, and the corresponding Cramer Rao Bound is called the conditional Cramer Rao bound. The conditional maximum likelihood estimator for the symbol timing delay has been derived in this thesis. The conditional Cramer Rao bound will be derived for the known data and

known channel system and for the unknown data and unknown channel system, and it will be used to measure the mean square error efficiency in the simulations.

The log-likelihood function used to find the conditional maximum likelihood estimator for the known data and known channel system is

$$\begin{aligned}&\Lambda(\tau, \mathbf{H}, \mathbf{A}) \\ &= C - \frac{1}{N_0} \sum_{m=1}^{N_R} \int_0^{T_0} \left( r_m(t) - \sum_{i=1}^{N_T} h_{m,i} s_i(t-\tau) \right) \left( r_m^*(t) - \sum_{i=1}^{N_T} h_{m,i}^* s_i^*(t-\tau) \right) dt.\end{aligned} \tag{2.86}$$

In equation (2.86), the signal transmitted from antenna $i$ is

$$s_i(t) = \sum_{k=-L_p}^{L_0+L_p-1} a_i(k)\, p(t - kT_s), \tag{2.87}$$

and the signal received at antenna $m$ is

$$\begin{aligned} r_m(t) &= \sum_{i=1}^{N_T} h_{m,i} s_i(t-\tau) + w_m \\ &= \sum_{i=1}^{N_T} \sum_{k=-L_p}^{L_0+L_p-1} h_{m,i} a_i(k)\, p(t - kT_s - \tau) + w_m \\ &= \sum_{k=-L_p}^{L_0+L_p-1} \alpha_m(k) p(t - kT_s - \tau) + w_m \end{aligned} \tag{2.88}$$

where

$$\alpha_m(k) = \sum_{i=1}^{N_T} h_{m,i} a_i(k). \tag{2.89}$$

The Cramer Rao bound is

$$E\left\{ |\tau - \tau_{ML}|^2 \right\} \geq \frac{1}{E\left\{ |\frac{\partial}{\partial \tau} \Lambda(\tau)|^2 \right\}}, \tag{2.90}$$

which can also be expressed as

$$E\left\{ |\tau - \tau_{ML}|^2 \right\} \geq -\frac{1}{E\left\{ \frac{\partial^2}{\partial \tau^2} \Lambda(\tau) \right\}}. \tag{2.91}$$

To use this definition of the Cramer Rao bound, the second derivative of the log-likelihood function with respect to $\tau$ must be found. The first derivative is

$$\begin{aligned}
&\frac{\partial}{\partial\tau}\Lambda\left(\tau,\mathbf{H},\mathbf{A}\right)=-\frac{1}{N_0}\sum_{m=1}^{N_R}\int_0^{T_0}\left(r_m\left(t\right)-\sum_{k=-L_p}^{L_0+L_p-1}\alpha_m(k)p\left(t-kT_s-\tau\right)\right)\\
&\times\left(\sum_{k=-L_p}^{L_0+L_p-1}\alpha_m(k)^*p'\left(t-kT_s-\tau\right)\right)dt\\
&-\frac{1}{N_0}\sum_{m=1}^{N_R}\int_0^{T_0}\left(\sum_{k=-L_p}^{L_0+L_p-1}\alpha_m(k)p'\left(t-kT_s-\tau\right)\right)\\
&\times\left(r_m^*\left(t\right)-\sum_{k=-L_p}^{L_0+L_p-1}\alpha_m(k)^*p\left(t-kT_s-\tau\right)\right)dt\\
&=-\frac{2}{N_0}\mathrm{Re}\left\{\sum_{m=1}^{N_R}\int_0^{T_0}\left(r_m\left(t\right)-\sum_{k=-L_p}^{L_0+L_p-1}\alpha_m(k)p\left(t-kT_s-\tau\right)\right)\right.\\
&\left.\times\left(\sum_{k=-L_p}^{L_0+L_p-1}\alpha_m(k)^*p'\left(t-kT_s-\tau\right)\right)dt\right\},
\end{aligned}\tag{2.92}$$

and the second derivative is

$$\begin{aligned}
&\frac{\partial^2}{\partial\tau^2}\Lambda\left(\tau,\mathbf{H},\mathbf{A}\right)=\frac{2}{N_0}\mathrm{Re}\left\{\sum_{m=1}^{N_R}\int_0^{T_0}\left(r_m\left(t\right)-\sum_{k=-L_p}^{L_0+L_p-1}\alpha_m(k)p\left(t-kT_s-\tau\right)\right)\right.\\
&\left.\times\left(\sum_{k=-L_p}^{L_0+L_p-1}\alpha_m(k)^*p'\left(t-kT_s-\tau\right)\right)dt\right\}\\
&-\frac{2}{N_0}\mathrm{Re}\left\{\sum_{m=1}^{N_R}\int_0^{T_0}\left(\sum_{k=-L_p}^{L_0+L_p-1}\alpha_m(k)p'\left(t-kT_s-\tau\right)\right)\right.\\
&\left.\times\left(\sum_{k=-L_p}^{L_0+L_p-1}\alpha_m(k)^*p'\left(t-kT_s-\tau\right)\right)dt\right\}.
\end{aligned}\tag{2.93}$$

Now, because

$$E\left[r_m\left(t\right)\right]=\sum_{k=-L_p}^{L_0+L_p-1}\alpha_m(k)p\left(t-kT_s-\tau\right),\tag{2.94}$$

the inverse of the Cramer Rao bound as defined in equation (2.91) is

$$\begin{aligned}
&- E\left[\frac{\partial^2}{\partial\tau^2}\Lambda\left(\tau,\mathbf{H},\mathbf{A}\right)\right] \\
&= \frac{2}{N_0}\mathrm{Re}\left\{\sum_{m=1}^{N_R}\int_0^{T_0}\left(\sum_{k=-L_p}^{L_0+L_p-1}\alpha_m(k)p'\left(t-kT_s-\tau\right)\right)\right. \\
&\left.\times\left(\sum_{k=-L_p}^{L_0+L_p-1}\alpha_m(k)^*p'\left(t-kT_s-\tau\right)\right)d\tau\right\} \\
&= \frac{2}{N_0}\mathrm{Re}\left\{\sum_{m=1}^{N_R}\sum_{k=-L_p}^{L_0+L_p-1}\sum_{k'=-L_p}^{L_0+L_p-1}\alpha_m(k)\alpha_m(k')^*\right. \\
&\left.\times\int_0^{T_0}p'\left(t-k'T_s-\tau\right)p'\left(t-kT_s-\tau\right)dt\right\} \\
&= \frac{2}{N_0}\mathrm{Re}\left\{\mathrm{trace}\left(\boldsymbol{\alpha}^{\mathcal{H}}\mathbf{D}\boldsymbol{\alpha}\right)\right\} \\
&= \frac{2}{N_0}\mathrm{trace}\left(\mathbf{A}^{\mathcal{H}}\mathbf{H}^{\mathcal{H}}\mathbf{D}\mathbf{H}\mathbf{A}\right),
\end{aligned} \tag{2.95}$$

where

$$D_{ij} = \int_0^{T_0} p'\left(t-iT_s-\tau\right)p'\left(t-jT_s-\tau\right)dt = D_{ji}. \tag{2.96}$$

Therefore the conditional Cramer Rao bound is given by

$$\mathrm{CCRB} = \frac{N_0}{2\mathrm{trace}\left(\mathbf{A}^{\mathcal{H}}\mathbf{H}^{\mathcal{H}}\mathbf{D}\mathbf{H}\mathbf{A}\right)}. \tag{2.97}$$

For the unknown channel and unknown data system, $\alpha_m(k)$ must be treated as nuisance parameters and included in the Fisher information matrix $\mathbf{J}$, which may be organized as

$$\mathbf{J} = \begin{bmatrix} J_{\tau\tau} & \mathbf{J}_{\tau\boldsymbol{\alpha}} \\ \mathbf{J}_{\boldsymbol{\alpha}\tau} & \mathbf{J}_{\boldsymbol{\alpha}\boldsymbol{\alpha}} \end{bmatrix} \tag{2.98}$$

where $\boldsymbol{\alpha} = \mathbf{H}\mathbf{A}$. $J_{\tau\tau}$ is the scalar given by (2.95). The submatrix $\mathbf{J}_{\tau\boldsymbol{\alpha}}$ has entries

$$\begin{aligned}
-\mathrm{E}\left\{\frac{\partial^2\Lambda\left(\tau,\mathbf{H},\mathbf{A}\right)}{\partial\tau\partial\alpha_m^*(k)}\right\} &= -\frac{1}{N_0}\sum_{k'=-L_p}^{L_0+L_p-1}\alpha_m(k')\int_0^{T_0}p'(t-k'T_s-\tau)p(t-kT_s-\tau)dt \\
&= -\frac{1}{N_0}\sum_{k'=-L_p}^{L_0+L_p-1}\alpha_m(k')R'(k'T_s+\tau,kT_s+\tau)
\end{aligned} \tag{2.99}$$

where $R'(k'T_s+\tau, kT_s+\tau)$ is an element of the matrix $\mathbf{R}'(\tau)$ defined by equation (2.20). The submatrix $\mathbf{J}_{\boldsymbol{\alpha}\tau} = \mathbf{J}_{\tau\boldsymbol{\alpha}}^{\mathcal{T}}$. The submatrix $\mathbf{J}_{\boldsymbol{\alpha}\boldsymbol{\alpha}}$ has entries

$$\begin{aligned} -\mathrm{E}\left\{\frac{\partial^2\Lambda(\tau,\mathbf{H},\mathbf{A})}{\partial\alpha_m(k)\partial\alpha_{m'}^*(k')}\right\} &= \delta_{m,m'}\times\frac{1}{N_0}\int_0^{T_0} p(t-kT_s-\tau)p(t-k'T_s-\tau)dt \\ &= \delta_{m,m'}\times\frac{1}{N_0}R(kT_s+\tau,k'T_s+\tau) \end{aligned} \tag{2.100}$$

where $R(kT_s+\tau, k'T_s+\tau)$ is an element of the matrix $\mathbf{R}(\tau)$ defined by equation (2.9). The Cramer Rao bound is the upper left entry in the matrix $\mathbf{J}^{-1}$ which may be expressed as

$$\mathrm{E}\left\{|\tau-\tau_{ML}|^2\right\} \geq \frac{1}{J_{\tau\tau}-\mathbf{J}_{\tau\boldsymbol{\alpha}}\mathbf{J}_{\boldsymbol{\alpha}\boldsymbol{\alpha}}^{-1}\mathbf{J}_{\boldsymbol{\alpha}\tau}}. \tag{2.101}$$

The element of $\mathbf{J}_{\boldsymbol{\alpha}\boldsymbol{\alpha}}^{-1}$ corresponding to $\partial\Lambda(\tau,\mathbf{H},\mathbf{A})/\partial\alpha_m(k)\partial\alpha_{m'}^*(k')$ can be expressed as $N_0\delta_{m,m'}R^{-1}(k,k')$ where $R^{-1}(k,k')$ is the $k$-th row and $k'$-th column of $\mathbf{R}^{-1}(\tau)$. The required matrix product may be expressed as

$$\begin{aligned} \mathbf{J}_{\tau\boldsymbol{\alpha}}\mathbf{J}_{\boldsymbol{\alpha}\boldsymbol{\alpha}}^{-1}\mathbf{J}_{\boldsymbol{\alpha}\tau} &= \frac{2}{N_0}\mathrm{Re}\left\{\sum_{m=0}^{N_R-1}\sum_{k'}\sum_{k}\sum_{l'}\sum_{l}\alpha_m(l)R'(kT_s+\tau,lT_s+\tau)\right. \\ &\quad\left.\times\alpha_m^*(l')R'(k'T_s+\tau,l'T_s+\tau)R^{-1}(k,k')\right\} \\ &= \mathrm{trace}\left(\boldsymbol{\alpha}^{\mathcal{H}}\mathbf{R}'^{\mathcal{T}}(\tau)\mathbf{R}^{-1}(\tau)\mathbf{R}'(\tau)\boldsymbol{\alpha}\right) \\ &= \mathrm{trace}\left((\mathbf{H}\mathbf{A})^{\mathcal{H}}\mathbf{R}'^{\mathcal{T}}(\tau)\mathbf{R}^{-1}(\tau)\mathbf{R}'(\tau)(\mathbf{H}\mathbf{A})\right). \end{aligned} \tag{2.102}$$

Thus, the conditional Cramer Rao bound for the unkown data and unknown channel maximum likelihood symbol timing delay estimator may be expressed as

$$\mathrm{E}\left\{|\tau-\tau_{ML}|^2\right\} \geq \frac{N_0}{2\times\mathrm{trace}\left((\mathbf{H}\mathbf{A}^{\mathcal{H}}\left[\mathbf{D}(\tau)-\mathbf{R}'^{\mathcal{T}}(\tau)\mathbf{R}^{-1}(\tau)\mathbf{R}'(\tau)\right]\mathbf{H}\mathbf{A}\right)} \tag{2.103}$$

where $\mathbf{D}(\tau)$ is given by (2.96) and $\mathbf{R}'(\tau)$ by (2.20).

## 2.3 Simulations

### 2.3.1 A Block Processing Structure

The ML timing estimators (2.10), (2.29), and (2.52) and their corresponding approximations (2.12), (2.28), and (2.53), respectively, require computation of the

matched filter outputs $\mathbf{x}_m(\tau)$ at the output of each receive antenna as a function of the unknown symbol timing delay $\tau$. Since there is no closed-form expression for $\tau_{ML}$ in terms of the received signals, the estimation algorithm must "search" for the symbol timing delay that maximizes the appropriate likelihood function. This search may be either sequential or parallel. The sequential search is described in chapter 3. A parallel search is the most appropriate search when using block processing.

Ideally, the parallel search computes the vectors $\mathbf{x}_m(\tau)$ for *all* possible values of $\tau$ in parallel, computes the corresponding arguments in equations (2.10)-(2.12), (2.29)-(2.28), or (2.52)-(2.53), and selects the value of $\tau$ with the maximum output. In practice, $\tau$ is quantized to $Q$ parts/symbol so that only $Q$ vectors of matched-filter outputs $\mathbf{x}_m(0), \mathbf{x}_m(1/Q), \ldots, \mathbf{x}_m((Q-1)/Q)$ are computed in parallel [15, 16, 17]. The corresponding $Q$ values of the arguments of (2.10)-(2.12), (2.29)-(2.28), or (2.52)-(2.53) are computed. This thesis calls these values $\Lambda(0), \Lambda(1/Q), \ldots, \Lambda((Q-1)/Q)$ for brevity. Depending on the degree of accuracy required, the estimate can be formed either by simply setting $\tau_{ML}$ to the multiple of $1/Q$ corresponding to the largest $\Lambda(\cdot)$ or by using the values of $\Lambda(\cdot)$ with an interpolator to approximate a symbol timing delay with greater resolution. Usually, timing synchronization algorithms use a polynomial-based interpolator [10, 17, 20, 21] to keep computational complexity manageable. The value of $Q$ and the degree of the interpolating polynomial give the system designer a rich set of possibilities in the trade-off between computational complexity and performance.

An efficient way to produce the $Q$ vectors of matched filter outputs at each antenna in a sampled-data receiver is to use a polyphase filterbank as described in [22]. Assuming each subfilter is to operate at an equivalent sample rate of $N$ samples/symbol, a prototype pulse shape filter is generated at $Q > N$ samples/symbol. This thesis defines

$$p\left(l'\frac{T_s}{Q}\right) \quad \text{for} \quad -L_pQ \leq l' \leq L_pQ \tag{2.104}$$

to represent the samples of the pulse shape. The polyphase decomposition of $p(l'T_s/Q)$ consists of a set of $Q$ subfilters, $p_0(lT_s/N), p_1(lT_s/N), \ldots, p_{Q-1}(lT_s/N)$ operating at $N$ samples/symbol. Each subfilter is obtained from $p\left(l'\frac{T_s}{Q}\right)$ by taking every $Q/N$-th

sample and starting from a different sample. The $q$-th subfilter is

$$p_q\left(l\frac{T_s}{N}\right) = p\left(l\frac{T_s}{N} + \frac{qT_s}{Q}\right) \quad \text{for} \quad -L_pN \leq l \leq L_pN \tag{2.105}$$

for $q = 0, 1, \ldots, Q-1$. Note that zeros should be appended to the end of each filter as needed to make all filters the same length. The polyphase filterbank consisting of $Q$ matched filters $h_0(lT_s/N), h_1(lT_s/N), \ldots, h_{Q-1}(lT_s/N)$ operating at $N$ samples/symbol is formed by setting $h_q(lT_s/N)$ equal to the time reversed version of $p_q(lT_s/N)$ for $q = 0, 1, \ldots, Q-1$.

A block diagram summarizing these ideas is illustrated in Figure 2.1. The complex baseband output from each of the $N_R$ receive antennas is sampled at a rate equivalent to $N$ samples/symbol. These samples are processed by the polyphase matched filter bank to produce $Q$ parallel matched filter output data streams at each of the receive antennas. These data streams are processed and combined as required by equations (2.10)-(2.12), (2.29)-(2.28), or (2.52)-(2.53) for each value of the quantized delay. These values are used to estimate the timing delay as described above.

### 2.3.2 Simulation Results

As a simple example demonstrating the polyphase filter approach, consider a $4 \times 4$ MIMO system where the common modulation format is QPSK using the square-root raised cosine pulse shape with a roll-off factor of 50%. The square-root raised cosine impulse response is defined to have a delay of 6 symbols. The sample rate is $N = 2$ samples/symbol and the symbol timing delay is set to a percentage of the symbol period. The block processing structure is used. The training sequence length is defined as $L_0 = 32$ symbols.

A polyphase filter bank is used to calculate the mean square error for different values of $\tau$. This is a different method than that used in [13], where a pulse matrix is used in the MIMO system instead of using the matched filter outputs. Figure 2.2 shows a comparison of the log likelihood functions for these two methods. The curve of the log likelihood function using matched filter outputs is the same as the curve

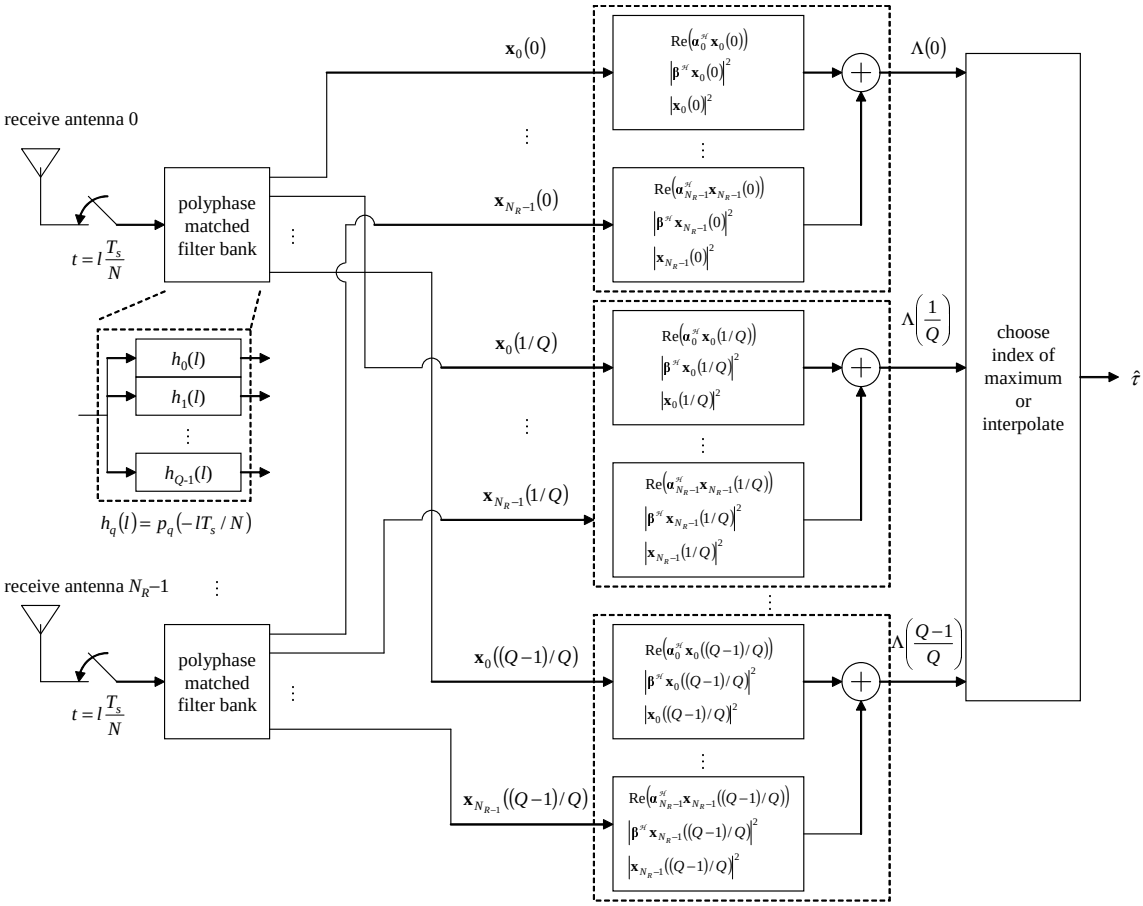


Figure 2.1: A block diagram illustrated the block processing for timing estimation in a sampled data MIMO receiver. A polyphase matched filter bank produces parallel outputs corresponding quantized values of the unknown timing delay. The matched filter outputs corresponding to each receive antenna are used to compute the argument of the function to maximized. Only the approximate forms for the three log-likelihood functions have been shown for simplicity.

of log likelihood function using the pulse matrix. For a large training sequence, the approximate maximum likelihood estimate for the known data and unknown channel system in equation (2.29) can be used. The curve for the approximate log likelihood function is also plotted in Figure 2.2. The curve of the approximation for the matched filter outputs is very close to the other two curves. The maximum likelihood estimates for all three curves would be very close because their maximum values are very close together.

A non-random channel matrix $\mathbf{H}$, which was measured in the Clyde building of Brigham Young University,

$$\mathbf{H} = \begin{bmatrix} 0.3385 & -0.0200 + j0.1639 & -0.0024 - j0.1449 & -0.3916 + j0.1087 \\ 0.0548 + j0.1172 & 0.1797 + j0.0034 & 0.1158 - j0.1729 & -0.0586 + j0.2624 \\ -0.3275 + j0.2380 & 0.1234 - j0.2448 & 0.0749 - j0.0607 & -0.0643 + j0.0024 \\ 0.1760 + j0.1558 & -0.2824 + j0.2457 & -0.1618 + j0.0622 & -0.1320 + j0.1096 \end{bmatrix}, \tag{2.106}$$

and a Gaussian i.i.d. channel matrix were used to find mean square error measurements in simulations. By averaging the squared error of many maximum likelihood estimates, the mean square errors were obtained as shown in Figure 2.3, Figure 2.4, Figure 2.5 and Figure 2.6 for various values of $Q$. In order to measure the efficiency of the maximum likelihood estimators, the conditional Cramer Rao bound was plotted with the mean square errors.

Figure 2.3 and Figure 2.4 show the mean square error and conditional Cramer Rao bound for the unknown channel and data-aided maximum likelihood estimator. The simulations were run using both the BYU nonrandom channel and the Gaussian i.i.d. channel matrices for various values of $Q$ and different search procedures. Figure 2.5 and Figure 2.6 show the mean square error and conditional Cramer Rao bound for the unknown channel and non-data-aided maximum likelihood estimator using the same two channel matrices. These simulations were run for various values of $Q$ and different search procedures.

The performance of all the maximum likelihood estimators is able to reach the Cramer Rao bound if $Q$ is sufficiently high and interpolation is used. The fact that performance improves when interpolation is used was observed in the simulation results presented in [18, 19]. When the signal-to-noise ratio is high enough, estimation errors due to quantization and interpolator approximations dominate the mean square error performance. As a consequence, estimator performance exhibits an error floor. For the nearest neighbor searches, no interpolation error is present and the error floor can be approximated using the standard assumptions of uniformly distributed quantization error to produce

$$\mathrm{MSE}_{\mathrm{floor}} \approx \frac{1}{12} \times \left(\frac{1}{2Q}\right)^2. \tag{2.107}$$

The use of interpolation reduces the error floor as shown. In all four cases, the use of quadratic interpolation with $Q = 32$ produces performance that is very close to the Cramer Rao bound. The effect of the approximation $\mathbf{R}(\tau) = \mathbf{I}$ results in a negligible performance degradation for the case considered. The performance degradation increases as $L_0$ decreases or the excess bandwidth decreases. For fixed $L_0$, the performance degradation for smaller values of the excess bandwidth is still small. The estimator performance on both channels is very similar, although the performance is slightly better for the BYU MIMO channel (2.106). One possible explanation for the similarity is that the performance of the estimators is only weakly tied to the statistical properties of the channel.

By comparing the data-aided mean square errors and the non-data-aided mean square errors, it is evident that the mean square error for the data-aided timing estimator versus the signal to noise ratio ranged from $3 \times 10^{-4}$ down to about $2 \times 10^{-7}$. The mean square error for the non-data-aided timing estimator ranged from $3 \times 10^{-3}$ down to about $2 \times 10^{-6}$. Obviously, the mean square error for the data-aided timing estimator is lower than the mean square error for the non-data-aided timing estimator. Also, the mean square error for the data-aided timing estimator is closer to the conditional Cramer Rao bound than the mean square error for the non-data-aided

timing estimator. This shows that the efficiency of the data-aided maximum likleli-hood timing estimator is better than that of the non-data-aided maximum likelihood timing estimator. The error produced during estimation mostly comes from the noise. The difference in the efficiencies of the mean square errors for the two maximum like-lihood timing estimators is due to the difference between knowing the data or not. For the data-aided maximum likelihood timing estimator, the known data is used to estimate the unknown channel, but for the non-data-aided maximum likelihood tim-ing estimator, both the data and the channel are unknown. This causes extra error during the estimation.

Figure 2.7 and Figure 2.8 are plots of the mean square error versus the symbol timing delay for a fixed signal to noise ratio. Figure 2.7 plots the mean square error for the data-aided maximum likelihood timing estimator versus the symbol timing delay. Figure 2.8 plots the mean square error for the non-data-aided maximum likelihood timing estimator versus the symbol timing delay. In each figure, the mean square error is plotted for a signal to noise ratio of 10 dB and 20 dB. By changing the symbol timing delay from 0 to $0.9T_s$, the mean square error does not change significantly.

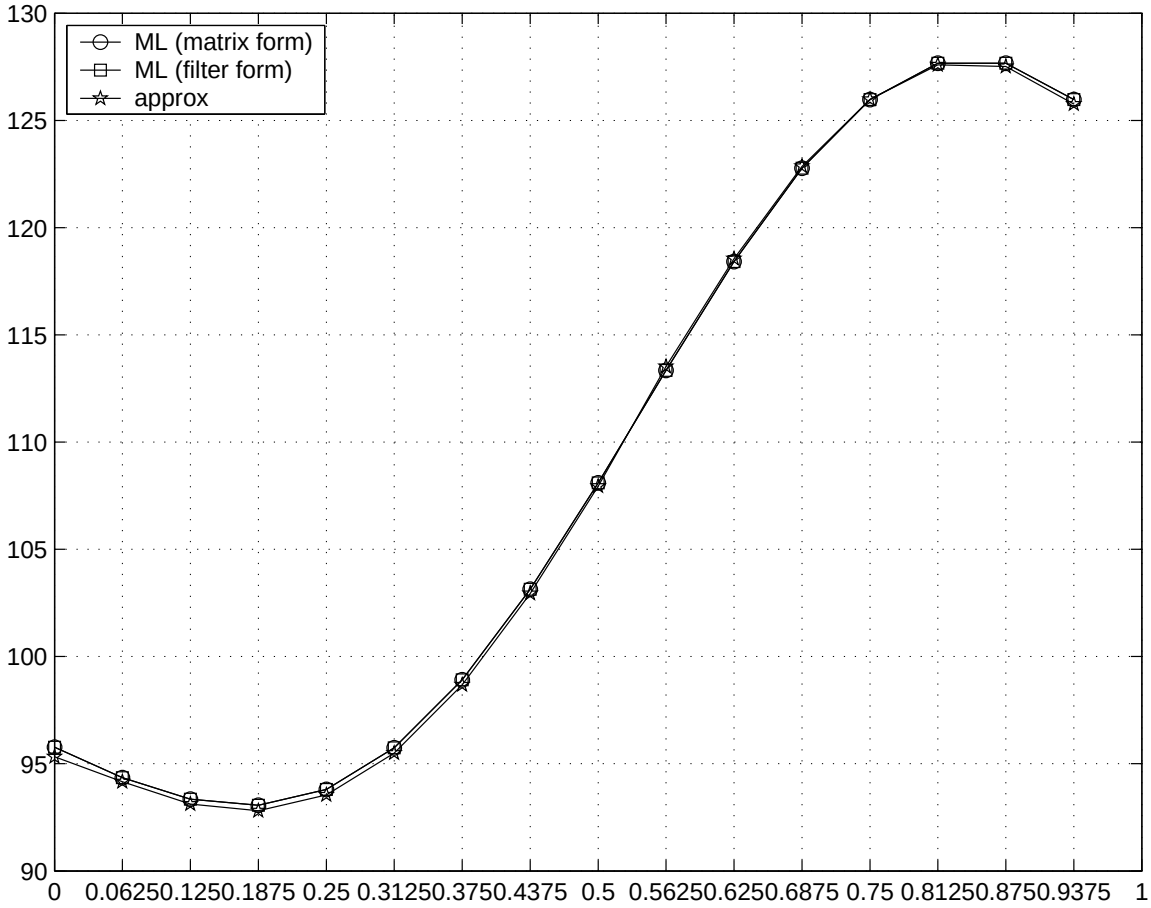


Figure 2.2: The compare of the maximum likelihood function of timing estimator corresponding to using polyphase filterbank outputs and using pulse matrix in [13].

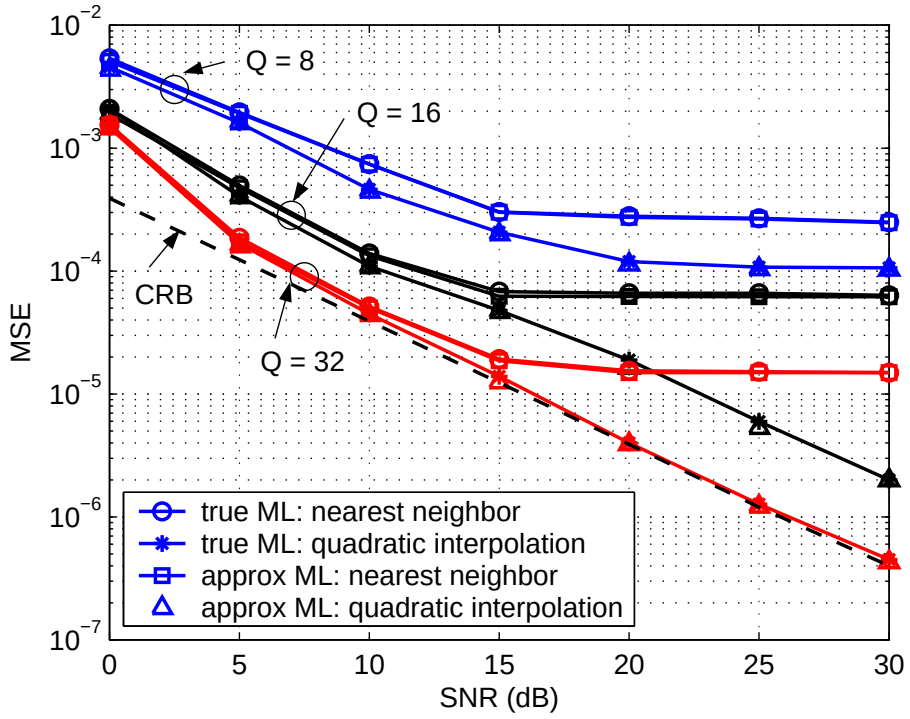


Figure 2.3: Simulation results for symbol timing estimation on an $N_T = 4$, $N_R = 4$ MIMO channel using QPSK with a square-root raised-cosine pulse shape with 50% excess bandwidth and $L_p = 6$. The channel matrix is given by (2.106). The true data-aided ML estimator is given by (2.26) and the approximate data-aided ML estimator is given by (2.28). Both nearest neighbor and quadratic interpolation searches were used with matched filters operating at $N = 2$ samples/symbol, $Q = 8, 16, 32$ and $L_0 = 32$.

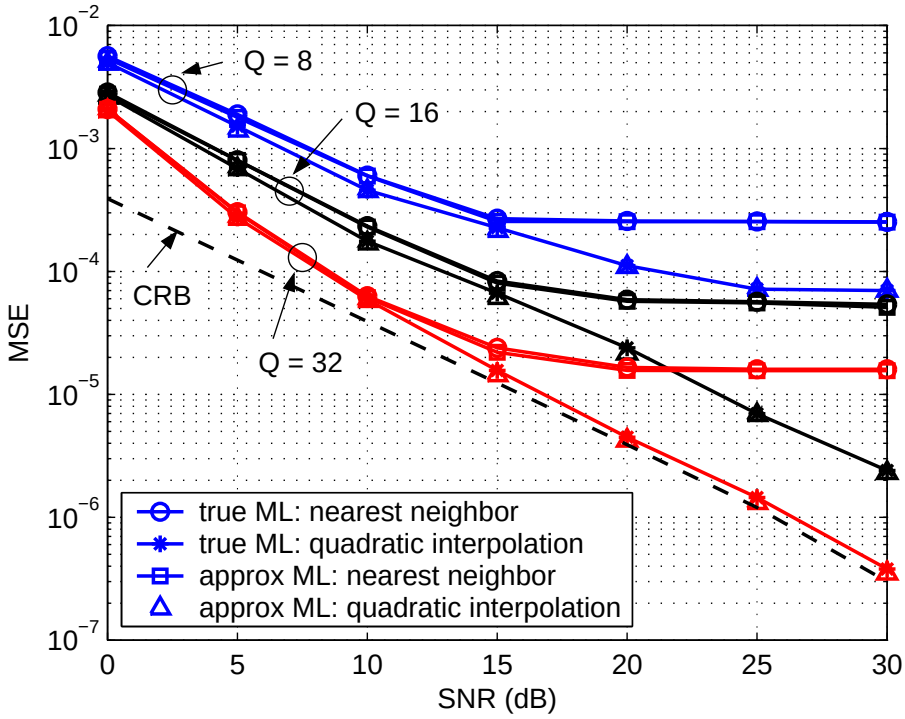


Figure 2.4: Simulation results for symbol timing estimation under the same conditions as those of Figure 2.3 except the channel matrix consists of independent, zero-mean complex Gaussian random variables with unit variance.

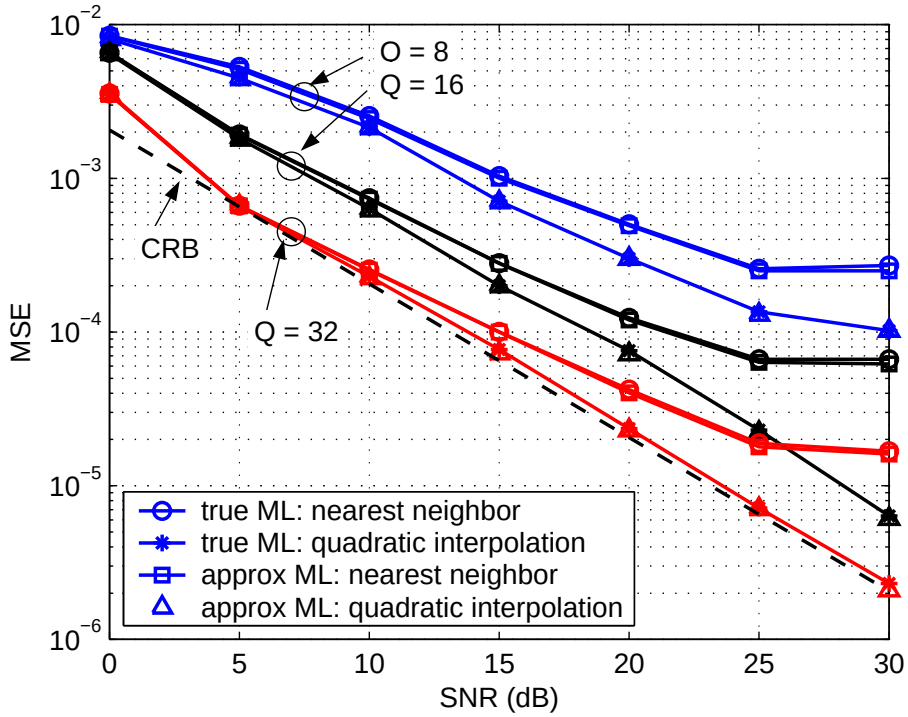


Figure 2.5: Simulation results for symbol timing estimation under the same conditions as those of Figure 2.3 except the true non-data-aided ML estimator (2.52) and the approximate non-data-aided ML estimator (2.53) are used.

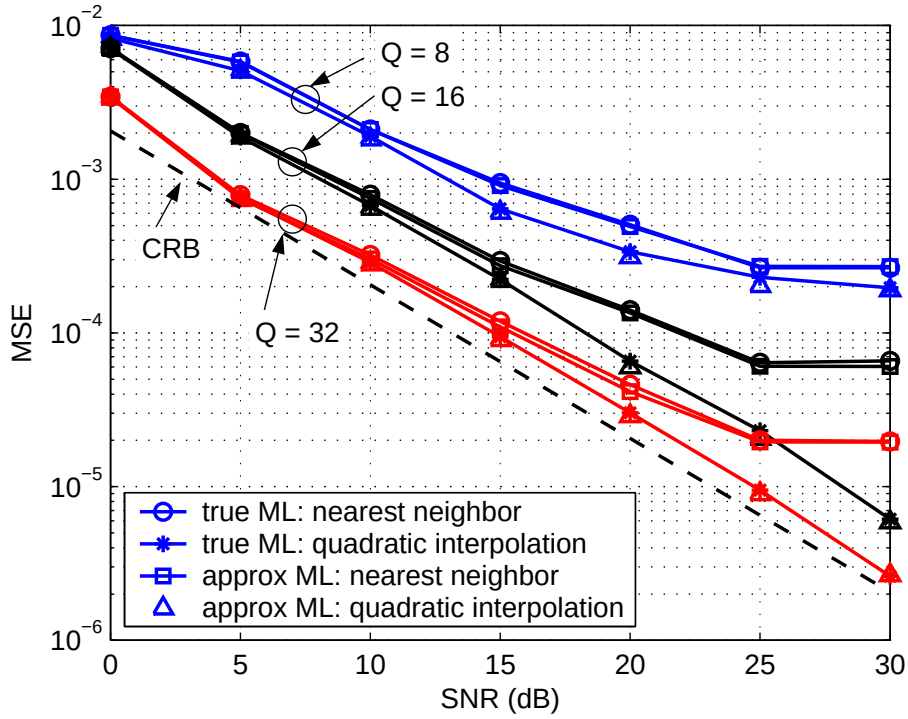


Figure 2.6: Simulation results for symbol timing estimation under the same conditions as those of Figure 2.5 except the channel matrix consists of independent, zero-mean complex Gaussian random variables with unit variance.

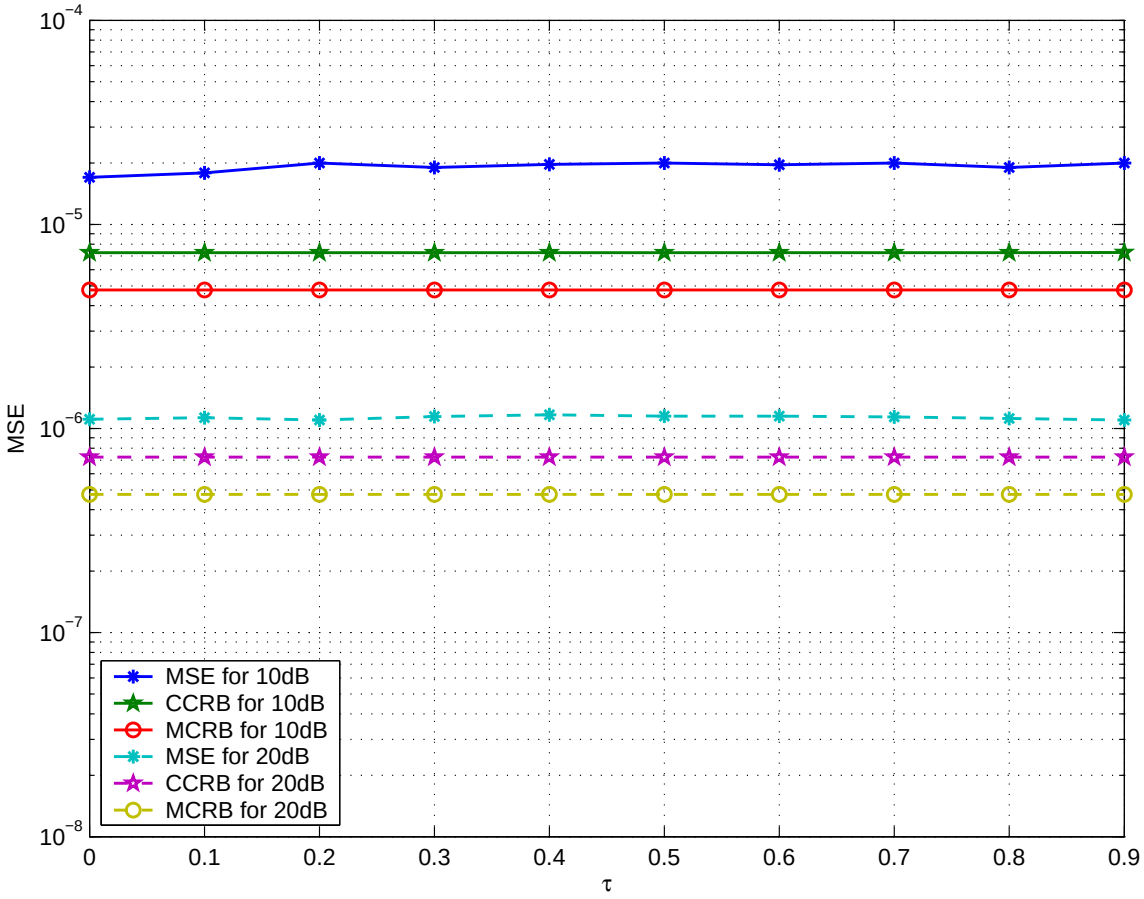


Figure 2.7: The mean square error of data-aided timing estimator versus the symbol timing delay.

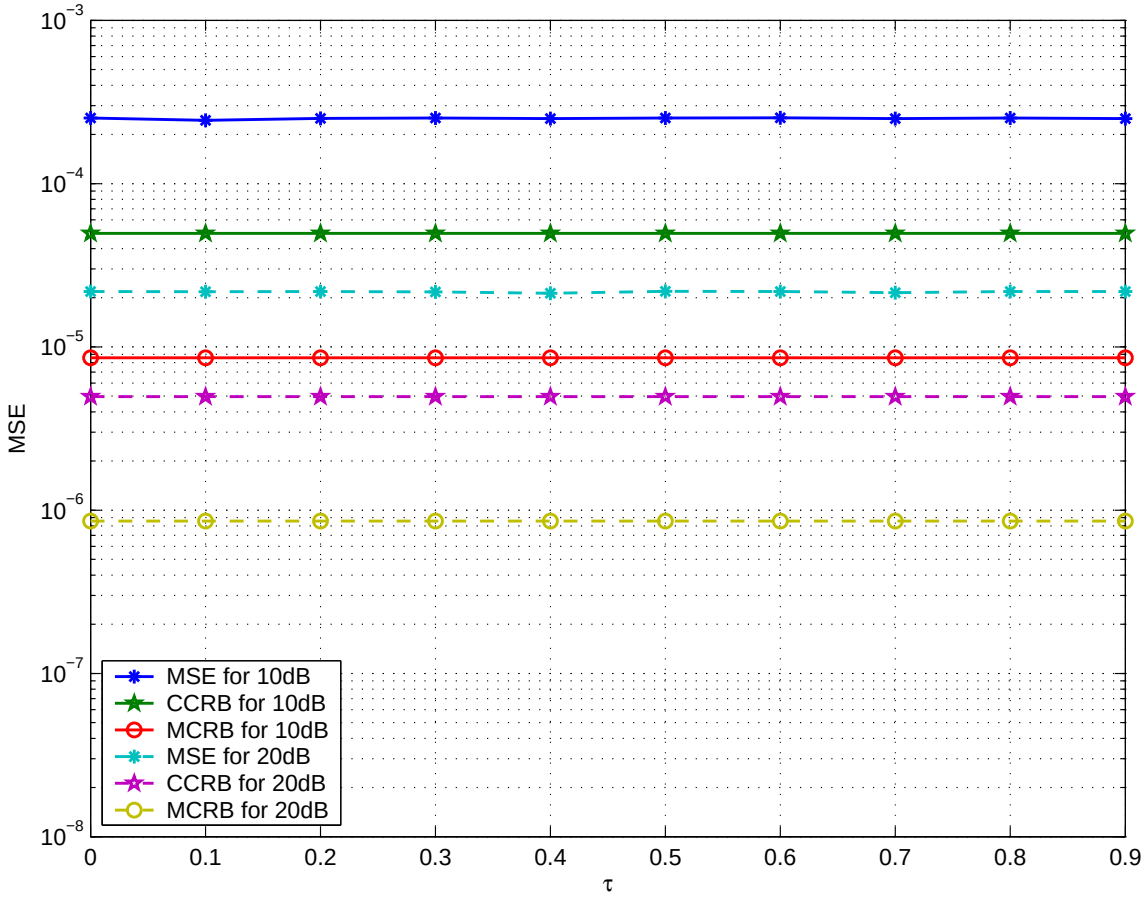


Figure 2.8: The mean square error of non-data-aided timing estimator versus the symbol timing delay.

# Chapter 3

# SEQUENTIAL PROCESSING

In a sequential search, it is usually more convenient to search for the value of $\tau$ that forces the derivative of the log-likelihood function with respect to $\tau$ to zero. An initial guess for $\tau$ is used to evaluate the derivative of the log likelihood function. If the derivative of the log-likelihood function is not zero, then $\tau$ is adjusted in the direction of the zero of the log-likelihood function. The sequential approach has the potential advantage that it is able to track differences between the data clock and the sampling (A/D) clock. Differences between these two time bases cause the interpolation interval to "slide through the data samples" as described in [21, 22]. This is probably not a problem in block processing if the data blocks are short enough that the symbol timing delay estimate is valid for the entire block. Sequential processing allows the observation interval to grow large, especially in the case of non-data-aided estimation.

The sequential search is usually implemented in the form of a discrete-time phase locked loop. A discrete-time phase locked loop is a feedback system that uses the derivative of the log-likelihood function as an error signal. The derivative log-likelihood function for the case of known data and either a known or an unknown channel is examined in Section 3.1, and the case of unknown data and unknown channel is examined in Section 3.2. Timing adjustments in the discrete time PLL were made using a piece-wise parabolic interpolator and a cubic interpolator. An example of the performance of the discrete-time phase-locked loop is made for the case of unknown data and unknown channel.

## 3.1 Sequential Timing Estimation with Known Data and Known/Unknown Channel

Computing the derivative of (2.5) with respect to $\tau$ and setting it equal to zero produces the following necessary condition for the ML estimate:

$$0 = \sum_{m=1}^{N_R} \left[ 2 \sum_{k=-L_p}^{L_0+L_p-1} \mathrm{Re}\left\{ \alpha_m^*(k) x'_m(kT_s + \tau_{ML}) \right\} - \sum_{k=-L_p}^{L_0+L_p-1} \sum_{k'=-L_p}^{L_0+L_p-1} \alpha_m(k) R'(kT_s + \tau_{ML}, k'T_s + \tau_{ML}) \alpha_{m'}^*(k') \right] \quad (3.1)$$

where $\alpha_m(k)$ is the $k$-th element of the vector $\boldsymbol{\alpha}_m$ defined by (2.89). This form of the estimator does not conveniently map to sequential processing. However, if $L_0$ is sufficiently long so that $\mathbf{R}(\tau) = \int_{T_0} \mathbf{P}(t;\tau)\mathbf{P}(t;\tau)^H dt = \mathbf{I}$, the second term on the right-hand-side of (3.1) can be dropped and the estimator assumes a form that is compatible with sequential processing:

$$0 = \sum_{m=1}^{N_R} \sum_{k=-L_p}^{L_0+L_p-1} \mathrm{Re}\left\{ \alpha_m^*(k) x'_m(kT_s + \tau_{ML}) \right\} \quad (3.2)$$

This simplified form permits an efficient implementation using a discrete-time phase-locked loop as illustrated in Figure 3.1(a). The time derivative of the matched filter outputs can be computed using a filter whose impulse response is the time derivative of the matched filter impulse response. In a continuous-time implementation, a voltage controlled clock (VCC) is adjusted to trigger the sampling of the output of the the continuous-time matched filter and derivative matched filter once per symbol as shown. In a discrete-time implementation, asynchronous samples of the received waveforms are processed by discrete-time matched filters and derivative matched filters operating at $N$ samples/symbol. Timing adjustment is performed using interpolators as described in [20, 21] or a polyphase filter bank for the matched filter and derivative matched filters as described in [22].

For the case of the known data and unknown channel system, the matrix form of the estimator (2.29) can be re-expressed using summations. Computing the

derivative of the argument of the resulting expression and setting it to zero produces

$$0 = \sum_{m=1}^{N_R} \sum_{k=-L_p}^{L_0+L_p-1} \mathrm{Re}\left\{ \sum_{i=1}^{N_T} a_i^*(k) x_m'(kT_s + \tau) \right\} \tag{3.3}$$

$$= \sum_{m=1}^{N_R} \sum_{k=-L_p}^{L_0+L_p-1} \mathrm{Re}\left\{ \beta^*(k) x_m'(kT_s + \tau) \right\} \tag{3.4}$$

where $\beta(k) = \sum_{i=1}^{N_T} a_i(k)$ is the sum of all the transmitted data symbols at symbol index $k$. A realization of a sequential search based on (3.4) is illustrated in Figure 3.1 (b).

## 3.2 Sequential Timing Estimation with Unknown Data and Unknown Channel

The approximate timing estimate (2.53) can be recast in a serial form that allows it to be easily incorporated into a phase-locked loop. Computing the derivative with respect to $\tau$ of the right-hand side of (2.53) and setting it equal to zero produces the necessary condition for the ML estimate:

$$0 = \sum_{m=1}^{N_R} \sum_{k=-L_p}^{L_0+L_p-1} \mathrm{Re}\left\{ x_m^*(kT_s + \tau_{ML}) x_m'(kT_s + \tau_{ML}) \right\}. \tag{3.5}$$

The use of (3.5) as an error signal in a phase-locked loop is illustrated in Figure 3.2.

An example of the performance of the discrete-time phase-locked loop is illustrated in Figures 3.5, 3.6 and 3.7 for the same $N_T = 4$, $N_R = 4$ MIMO channel from [24] used previously. Again, simulation of four separate QPSK signals using the square-root raised-cosine pulse shape with 50% excess bandwidth and $L_p = 6$ was used. A second order loop with loop bandwidth $= 0.0025/T_s$ and damping factor $\zeta = 1$ was used with a linear interpolator and matched filters and derivative matched filters operating at $N = 4, 8, 16$ samples/symbol. Loop control implemented using a decrementing modulo-one counter as described in [20]. The timing error detector gain was determined from the "S-Curve" plotted in Figure 3.4 for this channel and signal sets. The timing error detector gain is the slope of the S-Curve at $\tau_e = 0$ and is 0.05 the case of $N_T = 4$ random QPSK data streams with unit bit energy. Figure 3.3

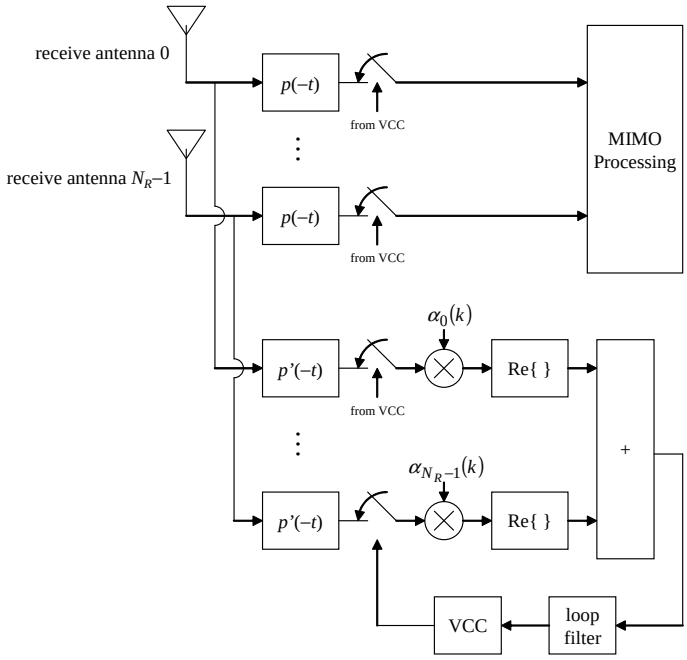


(a)

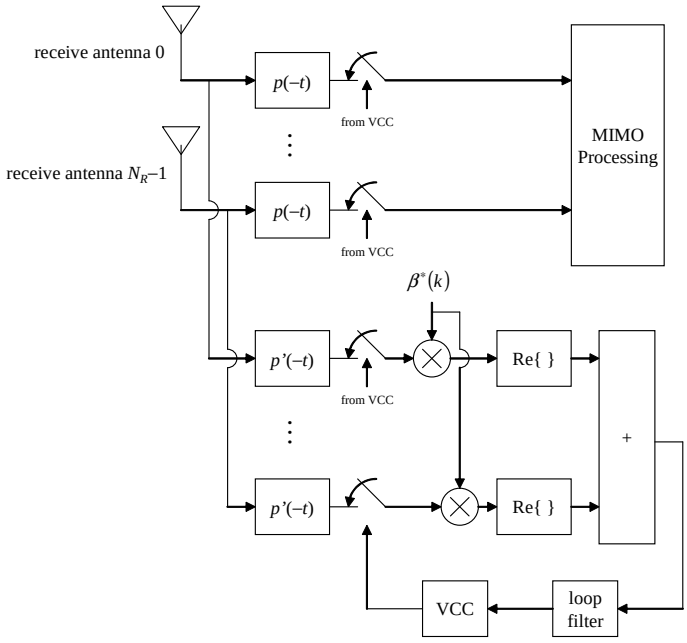


(b)

Figure 3.1: Sequential processing architecture based on the phase-locked loop for MIMO symbol timing synchronization. (a) PLL structure for the case of known channel and known data; (b) PLL structure for the case of unknown channel and known data.

is a block diagram of sequential processing based on the discrete-time phased-locked loop for symbol timing synchronization in a MIMO receiver. The fractional interpolation interval $\mu$ is plotted on the top of Figure 3.5 as a function of time. The middle plot of Figure 3.5 is a plot of the four symbol-spaced matched filter outputs after multiplication by $\mathbf{H}^{-1}$ corresponding to the first 250 symbol times. The lower plot of Figure 3.5 is a plot of the same corresponding to the last 250 symbol times. Observe that the loop locks after about 525 symbols (approximately 1.3 divided by the loop bandwidth as suggested in [23]) and that the effective signal-to-noise ratio on each of the channels is not identical. This is due to the eigenvalue spread of the matrix $\mathbf{H}^{\mathcal{H}}\mathbf{H}$.

Figure 3.6 and Figure 3.7 are plots of the timing error variance as a function of signal-to-noise ratio using parabolic interpolator and cubic interpolator. The Cramer Rao Bound (2.103) is also plotted for reference. Observe that the simulated mean-squared error reaches a floor at approximately $2 \times 10^{-5}$. It does not appear to be a function of N or the order of the interpolator. This suggests the error floor is not due to interpolator error, but rather self-noise in the phase-locked loop.

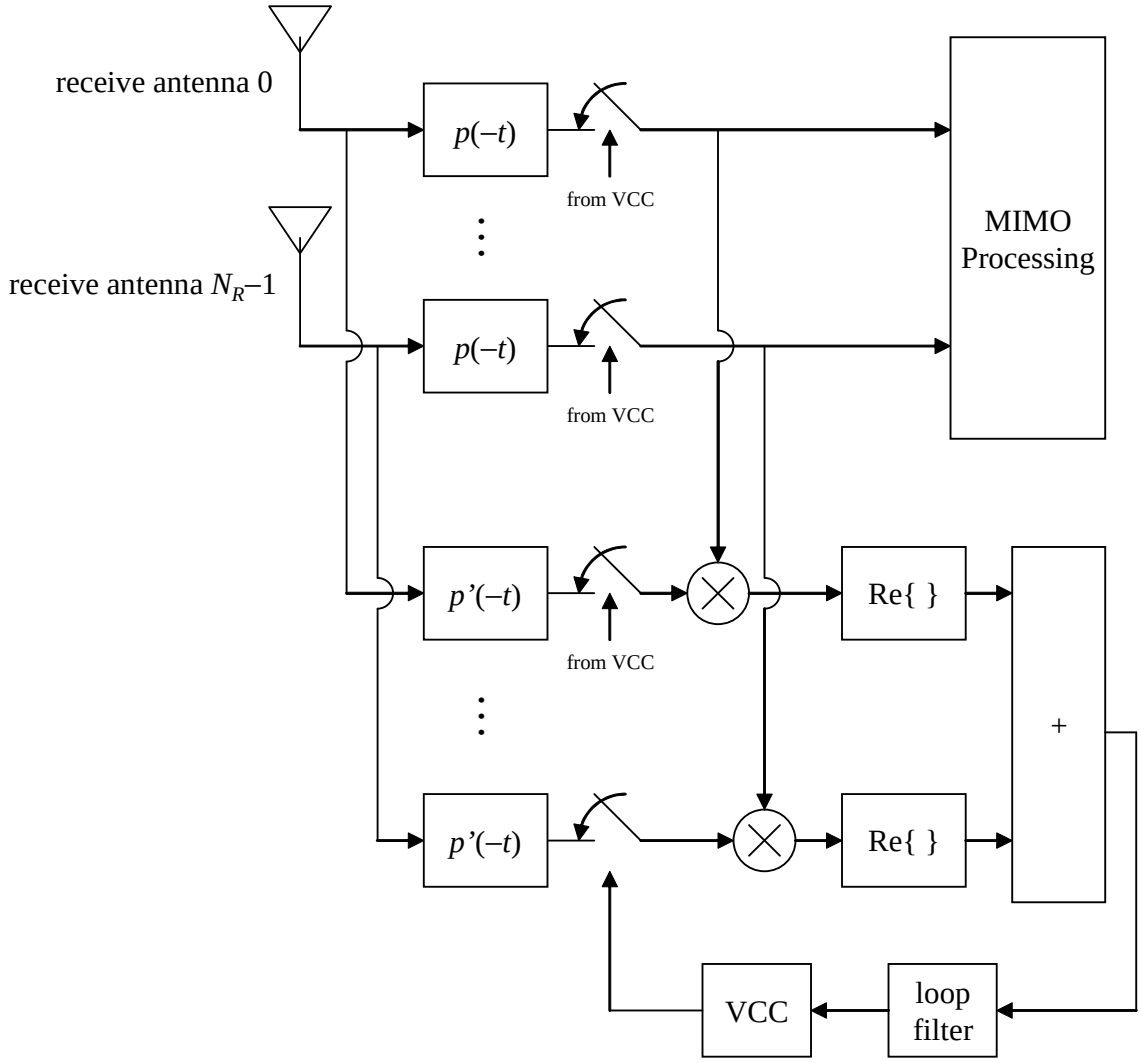


Figure 3.2: Sequential processing architecture based on the phase-locked loop for MIMO symbol timing synchronization for the case of unknown channel and unknown data.

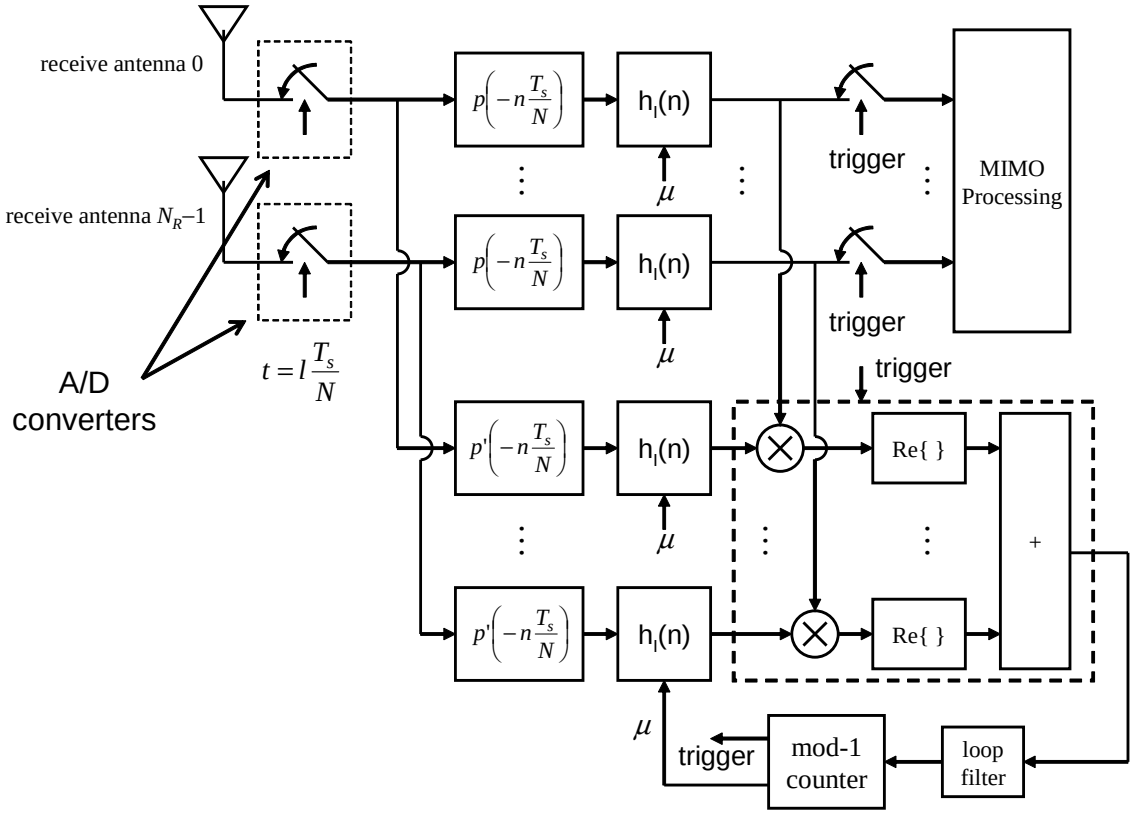


Figure 3.3: Sequential processing architecture based on the discrete-time phase-locked loop for MIMO symbol timing synchronization.

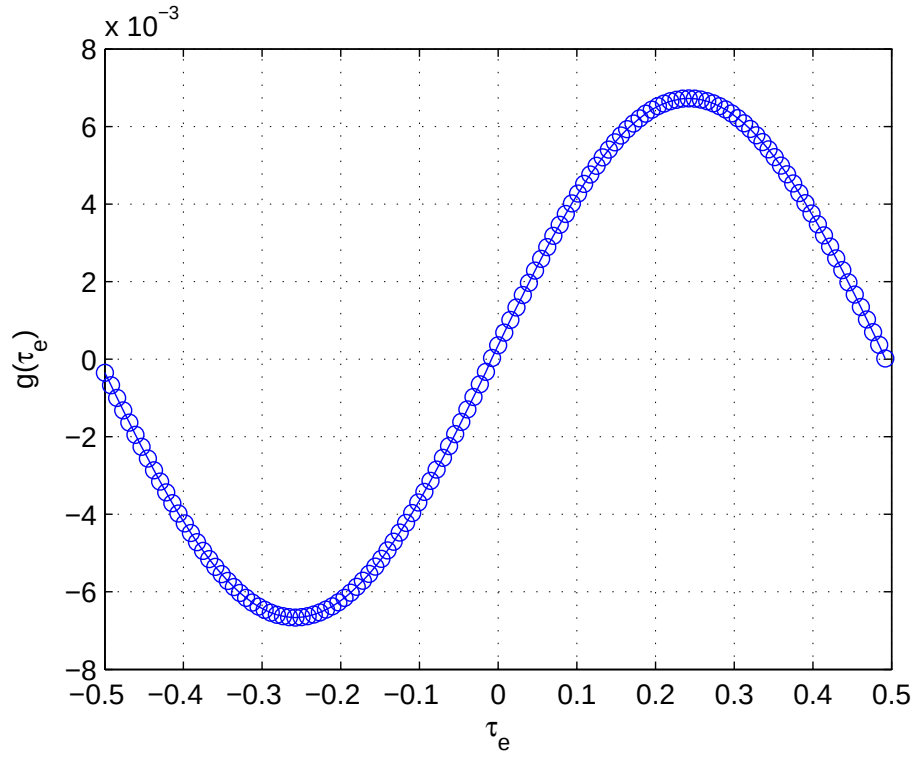


Figure 3.4: Timing error detector output or "S-Curve" for the timing error signal (3.5) over the $4 \times 4$ channel derived from [24] and using QPSK as a function of $\tau_e = \tau - \hat{\tau}$. The phase detector gain is the slope of the S-Curve at $\tau_e = 0$ and is 0.05 for this channel and $N_T = 4$ random QPSK data streams with unit bit energy and using a matched filter and derivative matched filters operating at $Q = 8$ samples/symbol.

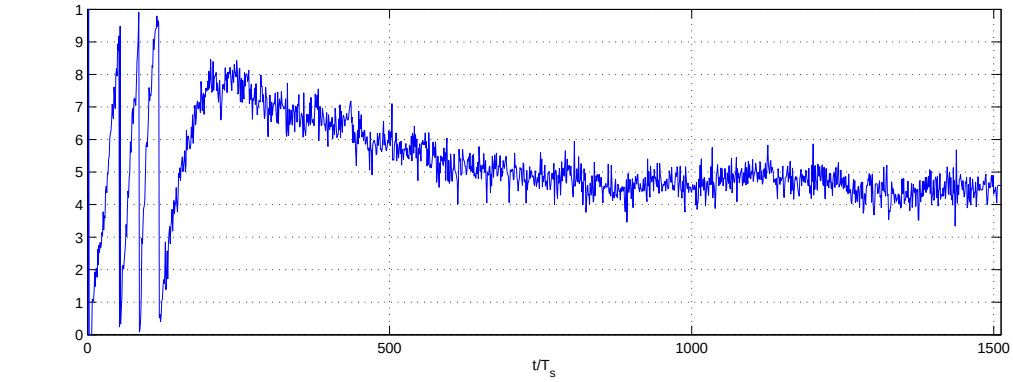


(a)

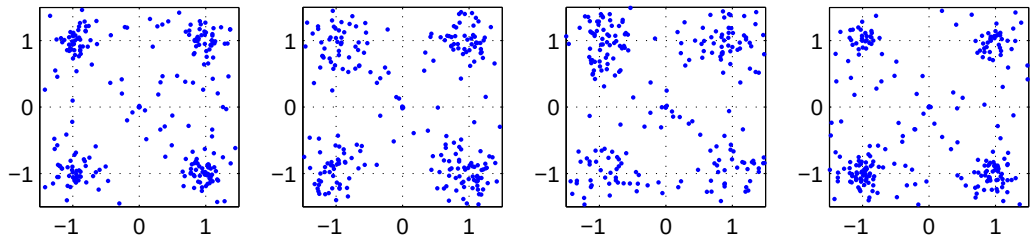

(b)

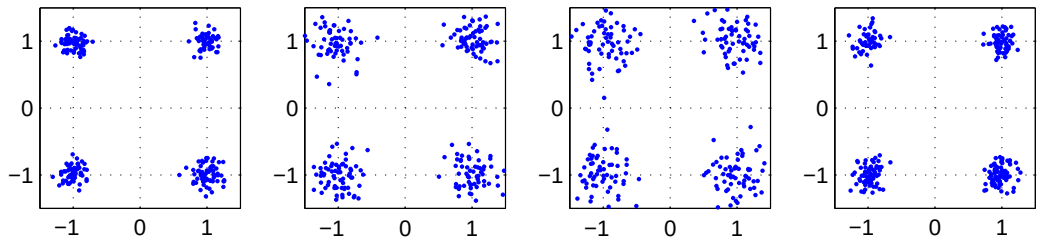

(c)

Figure 3.5: Examples of the PLL-based symbol timing synchronizer for the $4 \times 4$ MIMO channel from [24] using QPSK on each channel. The second order PLL operates at $N = 8$ samples/symbol, has a loop bandwidth of $0.0025/T_s$, and a damping factor of $\zeta = 1$, and uses a linear interpolator for timing adjustments. Four random QPSK data streams were simulated. (a) Plot of the fractional interpolation interval $\mu$ as a function of time. (b) Plot of the first 250 symbol-spaced matched filter outputs after multiplication by $\mathbf{H}^{-1}$. (c) Plot of the last 250 symbol-spaced matched filter outputs after multiplication by $\mathbf{H}^{-1}$

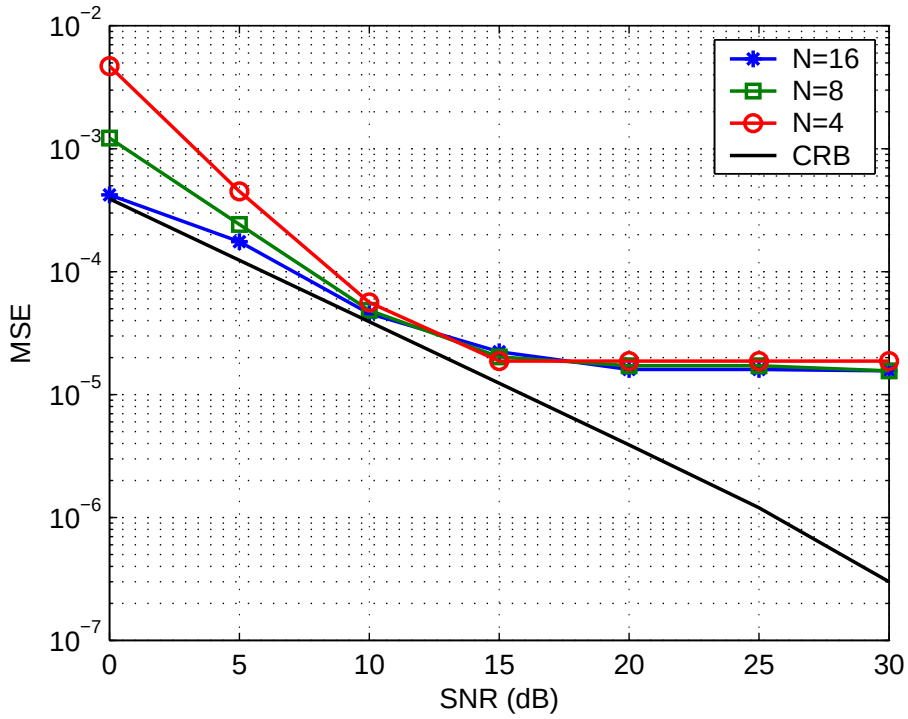


Figure 3.6: Simulated mean-squared error performance for the PLL-based timing estimator using the error signal (3.5). $N_T = 4$ random QPSK symbols were transmitted over the $N_T = 4$, $N_R = 4$ channel (2.106). The PLL is a second order loop with equivalent noise bandwidth 0.25% of the symbol rate and operating at $N = 4, 8, 16$ samples/symbol. Timing adjustments in the discrete-time PLL were made using a piece-wise parabolic interpolator.

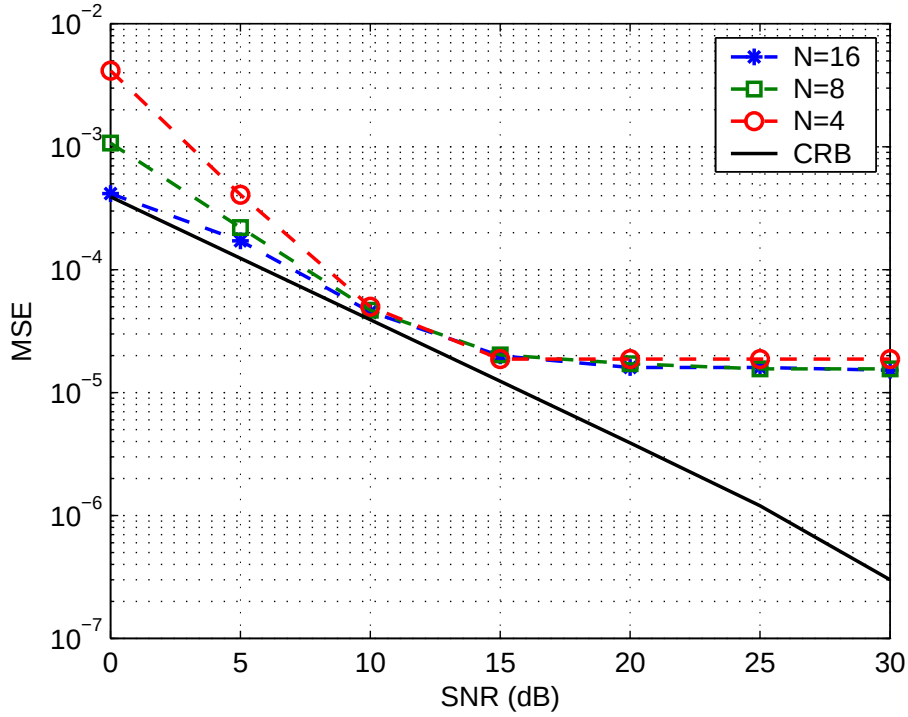


Figure 3.7: Simulated mean-squared error performance for the PLL-based timing estimator using the error signal (3.5). $N_T = 4$ random QPSK symbols were transmitted over the $N_T = 4$, $N_R = 4$ channel (2.106). The PLL is a second order loop with equivalent noise bandwidth 0.25% of the symbol rate and operating at $N = 4, 8, 16$ samples/symbol. Timing adjustments in the discrete-time PLL were made using a cubic interpolator.

# Chapter 4

# CONCLUSION

The maximum likelihood symbol timing delay estimators for a frequency non-selective MIMO channel assuming linear modulation are derived. The non-frequency selective fading assumption means the multipath delay spread is small, so the symbol timing delay is the same across all receive channels. The maximum likelihood estimator is similar in form to the maximum likelihood estimator for traditional SISO channels, but it differs in that it bases its estimate on weighted data from all of the transmit antennas.

Architectures based on both block processing and sequential processing are demonstrated and used in simulations. The block processing architecture is based on a $Q$-stage polyphase filterbank implementation of the derivative matched filter. A discrete time phase-locked loop is used for the sequential processing architecture.

There are four estimators. One estimator is for the known channel and known data system. The second estimator is for the unknown channel and known data system. The third estimator is for the known channel and unknown data system. The fourth estimator is for the unknown channel and unknown data system. When the channel is known and the data is unknown, the estimation can be handled in one of two ways: the conditional density (2.3) can be averaged over the assumed distribution of the channel gains using the total probability theorem, or the channel gains can be jointly estimated along with $\tau$. Solving for the channel gains and back-substituting into the likelihood function produces a likelihood function not explicitly dependent on $\mathbf{H}$. When both the channel and the data are unknown, the estimator can be implemented by treating the unknown channel matrix and unknown data matrix as

one unknown parameter, which can be jointly estimated along with $\tau$. By calculating the mean square error for the maximum likelihood estimators, their performance can be measured. The performance of the data-aided estimator was better than the performance of the non-data-aided estimator because the non-data-aided estimator treats both the channel and data as unknown parameters, which produces extra error during the estimation processes.

The approximate estimators published in [25] and [19] are special cases which use the approximate log likelihood functions and pulse matrix implementation instead of the matched filter outputs. The estimators based on block processing architectures can achieve the Cramer Rao bound when the number of quantization levels $Q$ is sufficiently high and interpolation is used. The performance of both the data-aided and non-data-aided estimators does not appear to be strongly dependent on the channel characteristics. Sequential processing using a discrete-time phase-locked loop was shown to achieve adequate performance.

## Bibliography


[1] S. Alamouti, "A simple transmit diversity technique for wireless communications," *IEEE Journal on Selected Areas in Communications*, vol. 16, no. 8, pp. 1451–1458, October 1988.

[2] V. Tarokh, H. Jafarkhani, and A. R. Calderbank, "Space-time block codes from orthogonal designs," *IEEE Transactions on Information Theory*, vol. 45, no. 5, pp. 1456–1467, July 1999.

[3] V. Tarokh, H. Jafarkhani, and A. R. Calderbank, "Space-time block coding for wireless communications: Performance results," *IEEE Journal on Selected Areas in Communications*, vol. 17, no. 3, pp. 451–460, March 1999.

[4] G. Raleigh and J. Cioffi, "Spatio-temporal coding for wireless communication," *IEEE Transactions on Communications*, vol. 46, no. 3, pp. 357–366, March 1998.

[5] V. Tarokh, N. Seshddri, and A. R. Calderbank, "Space-time codes for high data rate wireless communication: Performance criterion and code construction," *IEEE Transactions on Information Theory*, vol. 44, pp. 744–765, March 1998.

[6] V. Tarokh, A. Naguib, N. Seshadri, and A. R. Calderbank, "Space-time coding for high data rate wirless communication: Performance criteria in the presence of channel estimation errors, mobility, and multiple paths," *IEEE Transactions on Communications*, vol. 47, no. 2, pp. 199–207, February 1999.

[7] A. Naguib, V. Tarokh, N. Seshadri, and A. R. Calderbank, "A space-time coding modem for high-data-rate wireless communications," *IEEE Journal on Selected Areas in Communications*, vol. 16, no. 8, pp. 1459–1478, October 1988.

[8] J. Proakis, *Digital Communications*, McGraw-Hill, fourth edition edition, 2001.

[9] Henry. Stark and John. W. Woods, *Probability and Random Processes with Applications to Signal Processing*, Prentice Hall, third edition, 2002.

[10] U. Mengali and A. D'Andrea, *Synchronization Techniques for Digital Receivers*, Plenum, 1997.

[11] F. Harris and M. Rice, "Multirate digital filters for symbol timing synchronization in software defined radios," *IEEE Journal on Selected Areas in Communications*, vol. 19, no. 12, pp. 2346–2357, December 2001.

[12] Itsik. Bergel and Anthony J. Weiss, "Cramer-Rao Bound on Timing Recovery of Linearly Modulated Signals With No ISI" *IEEETransactions on Communications*,vol.51,April 2003.

[13] Jaume Riba, Josep Sala, and Gregori Vazquez, "Conditional Maximum Likelihood Timing Recovery: Estimatiors and Bounds," *IEEE Transactions on Signal Processing*, vol. 49, no. 4, pp. 835–850, April 2001.

[14] P. Stoica, and A. Nehorai, "Music, maximum likelihood and Cramer-Rao bound," *IEEE Transactions on Acoustics, Speech and Signal Processing*, vol. 37, pp. 720–741, May 1989.

[15] G. Ascheid and H. Meyr, "Maximum likelihood detection and synchronization by parallel digital signal processing," *in Proceedings of the IEEE Global Communications Conference*, vol. 2, pp. 32.2.1–32.2.5, 1984.

[16] G. Ascheid, M. Oerder, J. Stahl and H. Meyr, "An all digital receiver architecture for bandwidth efficient transmission at high data rates," *IEEE Transactions on Communications*, vol. 37, no. 8, pp. 804–813, August 1989.

[17] H. Meyr and G. Ascheid, "An all digital receiver architecture for bandwidth efficient transmission at high data rates," *IEEE Transactions on Communications*, vol. 37, no. 8, pp. 804–813, August 1989.

[18] Y.-C. Wu, S.-C. Chan, and E. Serpedin, "Symbol timing estimation in space-time coding systems based on orthogonal training sequences," *IEEE Transactions on Wireless Communications*, 2004, to appear.

[19] Y.-C. Wu and S.-C. Chan, "On the symbol timing recovery in space-time coding systems ," *in Proceeding of the IEEE Wireless Communications and Networking Conference*, vol. 1, New Orleans, LA, March 2003, pp. 420-424.

[20] F. M. Garnder, *Synchronization in Digital Communications*, New York ed. John Wiley & Sons, vol. 1, 1990.

[21] L. Erup, F. Garnder and R. Harris, "Interpolation in digital modems - part II: Implementation and performance," *IEEE Transactions on Communications*, vol. 41, no. 6, pp. 998–1008, June 1993.

[22] F. Harris, and M. Rice, "Multirate digital filters for symbol timing synchronization in software defined radios," *IEEE Journal on Selected Areas in Communications*, vol. 19, no. 12, pp. 2346–2357, December 2001.

[23] W. Waggener, *Pulse Code Modulation System Design*, Norwood, MA: Artech House, 1999.

[24] J. W. Wallace, M. A. Jensen, A. L. Swindlehurst, and B. D. Jeffs, "Experimental characterization of the MIMO wireless channel: Data acquisition and analysis," *IEEE Transactions on Antennas and Propagation*, 2004.

[25] A. Naguib, V. Tarokh, N. Seshadri and A. Calderbank, "A Space-Time Coding MODEM for High-Data-Rate Wireless Communications," *IEEE Journal on Selected Areas in Communication*, vol. 16, no. 8, pp. 1459–1478, October, 1998.